YERBİLİMLERİ
Bulletin for Earth Sciences

ISSN: 2687 - 2978

Yerbilimleri, 2020, 41 (2), 114-146, DOI:10.17824/yerbilimleri.701207

Hacettepe Üniversitesi Yerbilimleri Uygulama ve Araştırma Merkezi Bülteni

Bulletin of the Earth Sciences Application and Research Centre of Hacettepe University

Late Cretaceous to recent kinematic history of the Tuzgölü Basin, Central Anatolia, Turkey: a paleostress study

Tuzgölü Havzası'nın Geç Kretase-Günümüz arası kinematik evrimi (Orta Anadolu, Türkiye): Paleostres Çalışması

ERHAN GÜLYÜZ [1]

[1] *Van Yüzüncü Yıl University, Department of Geological Engineering, Van-Turkey*

Geliş (received): 9 Mart (March) 2020 Kabul (accepted) : 10 Ağustos (August) 2020

ABSTRACT

Traces of deformation events related to the Neotethyan and post-Neotethyan evolution of the Central Anatolia is well recorded in Upper Cretaceous to recent deposits of the Tuzgölü basin. In this regard, kinematic traces with age controls are crucial for differentiating and characterizing deformation phases that prevailed in the region. This study presents 57 paleostress inverse analysis based on more than 500 fault slip measurements collected from 41 different locations in the basin. The temporal distribution of the data sets indicates three different phases of deformation. The first one is represented by an almost E-W-directed compressional setting, which might be related to the late-stage closure of the Neo-Tethys Ocean and continental collision events along the Intra-Tauride Suture Zone during late Cretaceous to Oligocene time interval. The second phase is attributed to the segmentation of the Kırşehir block under NNW-SSE-directed compressional setting in the basin after the indentation of the Kırşehir block into the Pontide block along the İzmir-Ankara-Erzincan Suture Zone. The last phase is represented by the transtensional regime, which might be related to uplift of the entire Central Anatolian Plateau since ~ 10 Ma.

Key words: Paleostress, kinematic analyses, Tuzgölü Basin, Neotethys, Central Anatolia.

https://doi.org/10.17824/yerbilimleri.701207

E. GÜLYÜZ gulyuzerhan@gmail.com

[1] *Van Yüzüncü Yıl University, Department of Geol. Eng., Van-Turkey ORCID 0000-0002-1539-7982*

ÖZ

İç Anadolu'nun Neotetis ve Neotetis sonrası evrimi ile ilgili deformasyon olaylarının izleri, Geç Kretase – günümüz arası çökelim yaşına sahip Tuzgölü havzasının istiflerinde iyi bir şekilde kaydedilmiştir. Bu bağlamda, ilgili istifleri deforme eden ve yaş kontrollerine sahip kinematik izler, bölgede hakim olan deformasyon fazlarını ayırt ve karakterize etmek için oldukça önemlidir. Bu hedef doğrultusunda çalışma kapsamında, havza içindeki 41 farklı lokasyondan toplanmış olan 500'den fazla fay çiziği ölçümüne dayalı 57 paleostress ters çözümlemesi sunulmaktadır. İlgili ters çözümleme sonuçlarının zamansal dağılımı üç farklı deformasyon fazının ayırt edilmesine olanak sağlamıştır. Birinci faz, Neotetis Okyanusu'nun Geç Kretase-Oligosen zaman aralığı boyunca geç evre kapanımı ve İç Torid Kenet Kuşağı boyunca gerçekleşen kıta-kıta çarpışma olayları ile ilişkili neredeyse D-B doğrultulu bir sıkışma rejimi ile ilişkilendirilmiştir. İkinci faz, Kırşehir Bloğu'nun İzmir-Ankara-Erzincan Kenet Kuşağı boyunca Pontid bloğunun içine girintilenmesinden sonra Kırşehir Bloğu'nun segmentasyonu ile bağlantılı olabilecek KKB-GGD doğrultulu sıkışmalı rejimle ilişkilendirilmiştir. Son fazın ise, Orta Anadolu Platosu'nun ~ 10 My'dan bu yana yükselmesi ile ilişkili olabilecek transtansiyonal rejim ile alakalı olabileceği vurgulanmıştır.

Anahtar Kelimeler: *Paleostres, Kinematik analiz, Tuzgölü Havzası, Neotetis, Orta Anadolu.*

INTRODUCTION

Northward convergence of African and Arabian plates toward Eurasian plate since at least Cretaceous has resulted in the continental collision zones along different suture zones in the Central Anatolia due to closure of different branches of the Neo-Tethyan Ocean at different periods (Şengör and Yılmaz, 1981) (Figure 1). These are (i) İzmir-Ankara-Erzincan Suture Zone (IAESZ) creating a boundary between Gondwana-derived micro continents (Tauride-Anatolide platform and Kırşehir block) and the Sakarya-Pontide terrane of northern Turkey (Şengör and Yılmaz, 1981), and (ii) Inner Tauride suture zone (ITSZ) separating the northernmost tip of the African plate (Kırşehir Block, -a triangular tectonic zone belonging to African domain) from the main African continent. The timing of Neo-Tethyan ocean floor consumption beneath Eurasia along IAESZ is limited as middle Jurassic to late Cretaceous in the central Anatolia (Çelik et al., 2011; Okay et al., 2013; 2019). On the other hand, late Cretaceous fore-intra-arc and Paleocene-Oligocene foreland sequences of the southern Pontide margin are considered as the latest subduction and accretion products for the ocean (Tüysüz et al., 1995; Kaymakcı, 2000; Rice et al., 2006; 2009; Gülyüz et al., 2019).

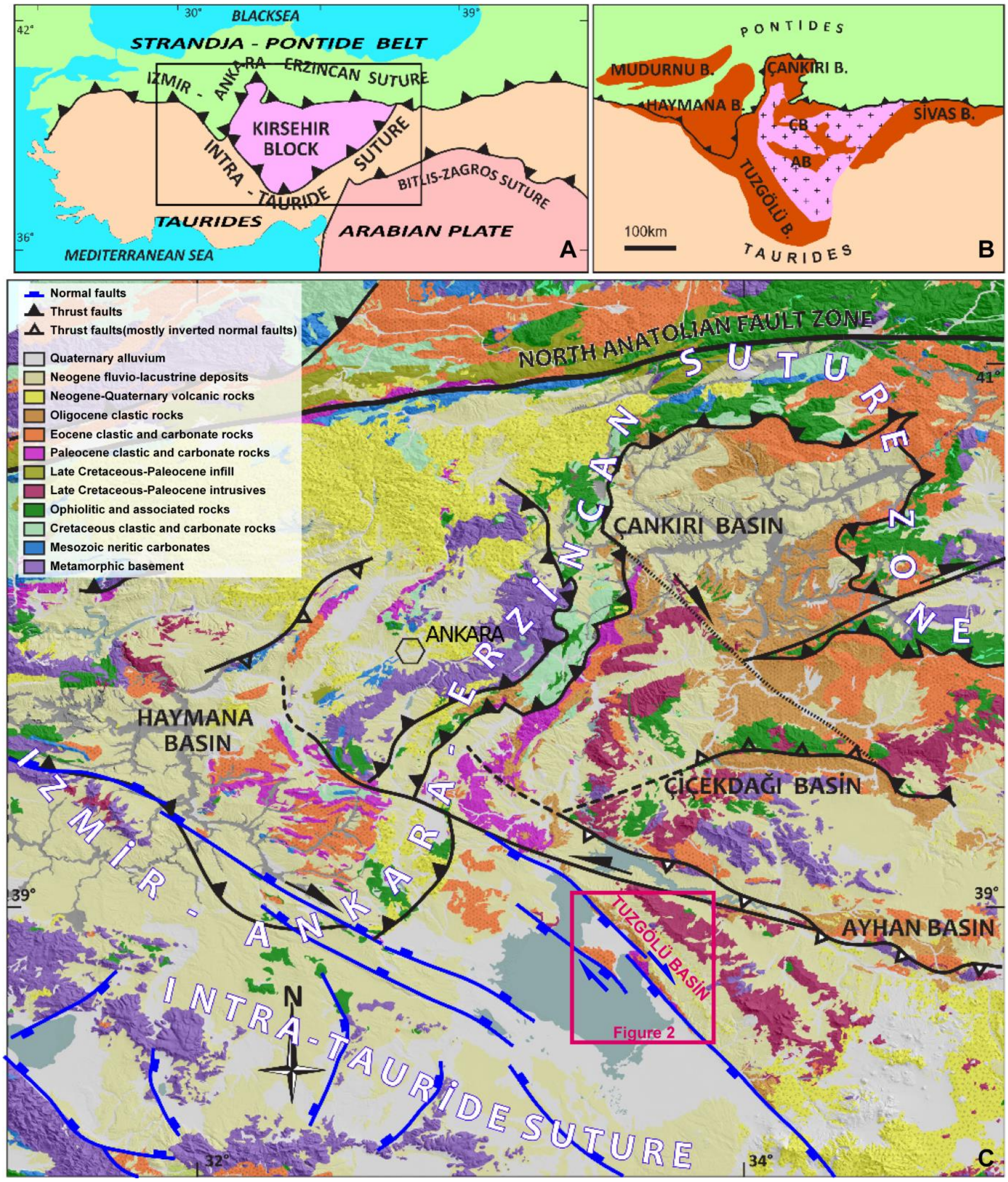

Figure 1. Geological setting of the Central Anatolia A) Tectonic divisions of Anatolia (modified from Görür et al., 1984); (B) Mesozoic and Cenozoic basins in central Anatolia, (modified from Görür et al., 1984, Özsayın and Dirik, 2007; Kaymakci, 2000; Kaymakci et al., 2009). (C) Geological map of the Central Anatolia (modified from MTA 2002 map).

Şekil 1. Orta Anadolu'nun jeolojik konumu A) Anadolu'nun tektonik bölümleri (Görür ve diğerleri, 1984'ten değiştirilmiştir); (B) Orta Anadolu'da bulunan Mesozoyik ve Senozoyik havzalar (Görür ve diğerleri, 1984, Özsayın ve Dirik, 2007; Kaymakçı, 2000; Kaymakçı ve diğerleri, 2009 çalışmalarından derlenmiştir). (C) İç Anadolu Jeoloji haritası (MTA 2002 haritasından değiştirilmiştir).

The time constraint is also supported by the blue-greenschist rocks of the Tauride Block with late Cretaceous to Paleocene burial ages and with almost same age arc-related magmatic rocks of northerly located Pontide Block (Okay, 1984; Okay et al., 1996; 2001; Candan et al., 2005; Pourteau et al., 2011; Kaygusuz et al., 2009; 2013; Öztürk et al., 2012; Speciale et al., 2014). Elongation of the subduction-related metamorphic rocks on Tauride Block follows the outline of the southern margin of Eurasian plate and southern margin of the Kırşehir Block (KB), which has a late Cretaceous-Paleocene age arc-related plutonic belt. The spatio-temporal relationship between the metamorphic rocks and arc-related rocks on the Kırşehir Block give way to infer (i) the existence of ITSZ (Erdogan et al., 1996; Kadıoğlu et al., 2006; Pourteau et al., 2011; 2013) as suggested by Görür et al. (1984) and (ii) a time constraint for the subduction beneath the Kırşehir block as late Cretaceous-Paleocene. Also, Lefevbre et al. (2013) suggest that the arc-related plutonic belt on the Kırşehir Block was in NNW-SSE trend which is parallel to the proposed elongation of the ITSZ. In this regard, the basins located within the Kırşehir Block and along the southern margin of it might be related to the evolution of the ITSZ system. In this context, (i) a marine basin directly located on the Kırşehir Block (Ayhan-Büyükkışla Basin) is defined as back-arc (extensional) to collisional basin (retro-arc foreland basin) for late Cretaceous to Paleocene and Eocene-Oligocene time intervals, respectively, and (ii) the basins located between the Kırşehir and Tauride Blocks are defined as with almost same analogy suggesting initially fore-arc (late Cretaceous-Paleocene) and latterly foreland basins (Eocene-Oligocene) (Görür et al., 1984; 1998; Clark and Robertson, 2002; Advokaat et al., 2014; Gülyüz et al., 2019). In contrast, all of these basins are defined as intra-continental basins by some other studies (e.g. Köksal and Göncüoğlu, 1997; Çemen et al., 1999; Dirik and Erol, 2003). However, existence of arc-related magmatic rocks on Kırşehir Block (Erdoğan et al., 1996; Kadıoğlu et al., 2006; Tüysüz et al., 1995) with Late-Cretaceous to Paleocene emplacement age (Erler et al., 1991; Erler and Göncüoğlu, 1996; Göncüoğlu, 1986; Whitney et al., 2003) and almost N-S elongation of these rocks for pre-Neogene time interval (Lefebvre et al., 2013) do not support the intra-continental origin for the basins. In this regard, Tuzgölü Basin, the main concern of this study, belongs to the ITSZ-related subduction-accretion system. In such a tectonic setting, Neo-Tethyan deformation phases in the basin are explained as extensional setting up to Middle Paleocene (Görür et al., 1984) or to Eocene (Çemen et al., 1999; Dirik and Erol., 2003; Gautier et al., 2008) followed by contractional setting up to Pliocene (Özsayın et al., 2013).

Post-Neotethyan evolution of the Anatolian landmass is characterized by two major tectonic processes. These are on-going convergence of Arabian plate since early?-late Miocene in the east (Burke and Şengör, 1986; Flerit et al., 2004; Gülyüz et al., 2020; Hüsing et al., 2009; Şengör et al., 1985), and a subduction system including a tear along the Hellenic and Cyprus trenches in the West (Le Pichon and Angelier, 1979; van Hinsbergen et al., 2010; Biryol et al. 2011). In general, these processes result in extension and contraction in the west and east, respectively (Şengör et al., 1985). The Central Anatolian plateau is located between these systems. One of the major responses of this tectonic configuration in the Central Anatolia is explained by CCW-block rotations supported by paleomagnetic (Kissel et al., 1993, 1987; Tatar et al., 1995; Gürsoy et al., 1998; 1999; 2003; 2011; Piper et al., 1996; 1997; 2010; Kaymakcı et al., 2003; Çinku, 2016, 2017; Hisarlı et al., 2016) and GPS (e.g Reilinger et al., 2006) data. In contrast to this homogenous rotation model, heterogeneous block rotations, accommodated by intra-continental strike-slip systems (e.g Savcılı and Delice-Kozalı fault zones) (Lefebvre et al., 2013), are suggested for the Central Anatolia. The activation of these fault zones is related to the compartmentalisation of the Kırşehir Block during its indentation into the Pontide block. The age control of the model is controlled by paleomagnetic sampling sites of the related study, which are limited only by Late Cretaceous to Paleocene intrusions. Therefore, the only constraint for the timing may only be suggested as post-Paleocene. The other deformation event for the Central Anatolia is described by drip tectonics model explaining the >1km uplift of the Central Anatolian plateau since ~10 Ma (after the compartmentalisation of the KB) (Göğüş et al., 2017). The outputs of the proposed model are roughly consistent with findings of Özsayın et al. (2013) indicating extension since ca. 6 Ma following the prior contraction in the region.

To sum up, the deformation history of Central Anatolia is basically explained by two periods related to Neotethyan and post-Neotethyan development of the region. Although there are numerous studies aiming to understand deformation style of the region since Late Cretaceous (e.g. Çemen et al., 1999; Görür et al., 1984; Özsayın et al., 2013), paleostress studies are limited and they only cover the post-Oligocene time interval. Studies giving results about the pre-Oligocene deformation history of the region are based on mainly low-quality seismic interpretations (e.g. Çemen et al., 1999; Fernandez-Blanco et al., 2013) or stratigraphic relations (Görür et al., 1984; 1998; Nairn et al., 2013) and do not present direct field evidence such as fault plane measurements or structural analyses. In this regard, this study aims to add new fault kinematic and structural data to the literature in order to shed some light on both Neotethyan and post-Neotethyan structural development of the Tuzgölü Basin.

Stratigraphic Background

The Tuzgölü Basin is represented by ~8 km-thick Upper Cretaceous to recent deposits (Dellaloğlu and Aksu, 1984; Aydemir and Ateş, 2006) (Figure 2a). NNW-SSE trending Upper

Cretaceous to Oligocene marine origin deposits of the basin are exposed in a narrow zone (<10km X ~130km) and they represent the Neo-Tethys portion of the basin system. These deposits are bounded by the hypothetic alignment of the ITSZ and Neogene cover deposits in the west. Their eastern boundary is also covered by Neogene continental deposits while the Late Cretaceous to Eocene arc-related Central Anatolian granitoids covered by the same units aligns in NNW-SSE (parallel to the marine units) direction which allows suggesting another hypothetic boundary between the basin and the active margin of the subduction system. Although a contact relationship between the basin and the basement rocks is observed neither in the field nor in the well data, the basement of the basin is accepted as Tauride block metamorphic rocks and accretionary complex products (mainly ophiolitic rocks) in the west and the Central Anatolian granitoids in the East (Arıkan, 1975; Dellaloğlu and Aksu, 1984; Görür et al., 1984; Çemen et al., 1999; Nairn et al., 2013). The contact relationship between the basement and marine units is inferred as unconformable (Arıkan, 1975; Dellaloğlu and Aksu, 1984) or tectonic (Görür et al., 1984; Çemen et al., 1999).

In contrast to blur inferences on the basement rocks, sedimentary sequences of the basin are relatively well-described. Upper Cretaceous to Oligocene deposits are represented by laterally and vertically transitional units. These units are described with different names in various studies (e.g. Righi and Cortesini, 1959; Akarsu, 1971; Arıkan, 1975; Derman, 1978; Dellaloğlu and Aksu, 1984; Görür et al., 1984; Çemen et al., 1999), therefore nomenclature on the units is complex. In this study, descriptions in the latest study (Çemen et al., 1999) are followed (Figure 2). In this regard, the oldest unit in the basin is represented by continental clastic of the Kartal Formation of which base is interpreted as basal conglomerates (Dellaloğlu and Aksu, 1984; Çemen et al., 1999). However, these conglomerates together with the rest of the formation may also be interpreted as marginal deposits. The Kartal formation grades into the Asmaboğazı formation, which is composed of shallow marine limestone layers. The distal equivalent of these formations is the Haymana Formation represented by green color mudstone-sandstone-conglomerate alternations. Fossil assemblages of these units are dated as late Cretaceous to Paleocene (Arıkan, 1975; Dellaloğlu and Aksu; 1984). The facies association of the units and their depositional time intervals indicate a depositional sequence containing almost the same age continental, shallow marine, and deeper marine units. This depositional sequence vertically grades into the upper sequence, which contains Paleocene Çaldağ, Kırkkavak and Karapınaryaylası formations, which are represented by reefal limestones, shallow marine limestone-marl-mudstone alternation, and deep marine turbidites, respectively.

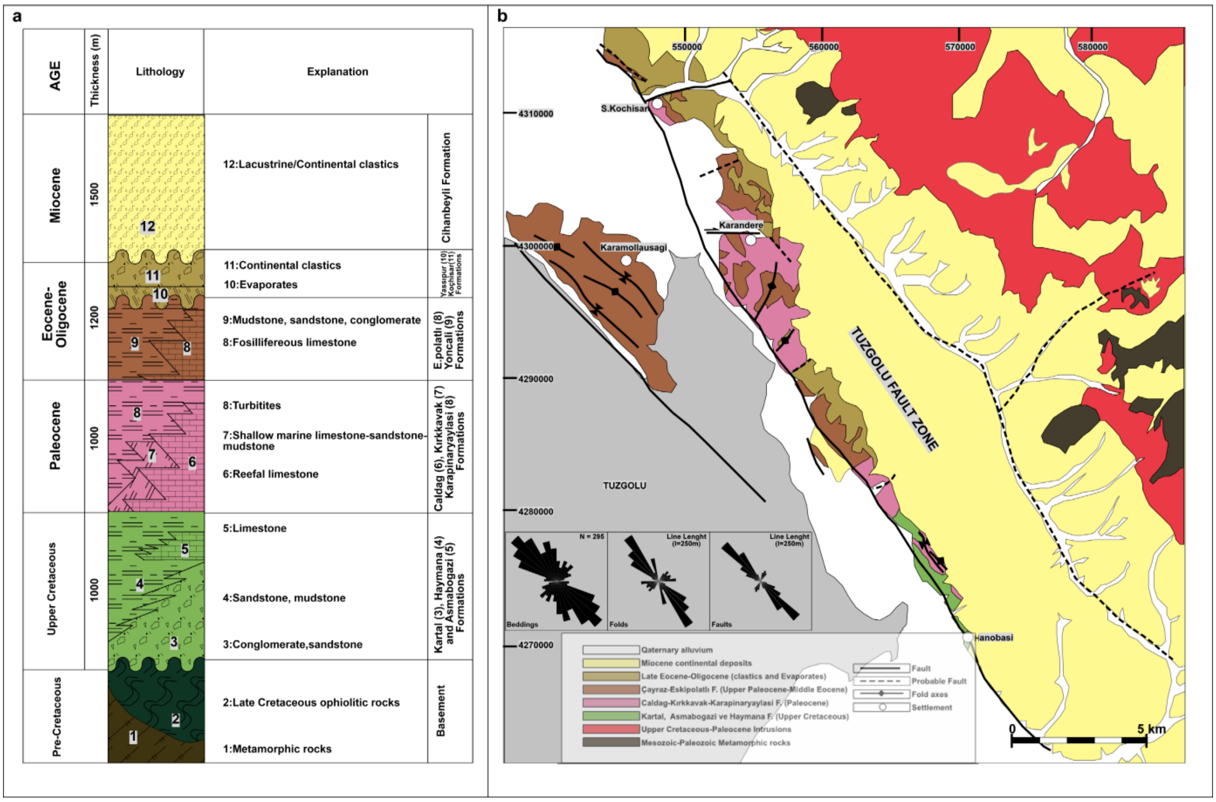

Figure 2. Columnar stratigraphic section of the Tuzgölü basin (modified from Çemen et al., 1999), (B) Geological map of the Tuzgölü basin. Rose diagrams represent (i) beddings measured in the basin (Appendix B), (ii) folds in basins (deforming marine deposits) and (iii) faults in the basin (Active faults).

Şekil 2. Tuzgölü havzasının stratigrafik kesiti (Çemen ve diğerleri, 1999'dan sonra modifiye edilmiştir), (B) Tuzgölü havzasının jeolojik haritası. Gül diyagramları: (i) havzada ölçülen tabakalanmaları (Ek), (ii) havzalardaki kıvrımları (deforme denizel birimleri etkileyen) ve (iii) havzadaki fayları (Aktif faylar) temsil eder.

This sequence also grades into Eocene sequence including shallow marine Yoncalı, calciturbitidic upper levels of the Karapınaryaylası and turbiditic Eskipolatlı formations. This entire marine or marine margin units are unconformably covered by Oligo-Miocene evaporates of Yassıpur Formation or continental clastics of Koçhisar/Gökdağ Formation. These continental deposits have unconformable relationship with the younger (Mio-Pliocene) Cihanbeyli formation represented by light color lacustrine/continental deposits.

METHODOLOGY

Field Studies and Data Collection

Field studies comprise observations/mapping of the major structures in the region and bedding measurements. Only the structures longer than 1 km, which are mainly Neogene structures, were mapped in the field or previous published maps were addressed. Bedding attitudes were collected only from the pre-Neogene units because the Neogene units are almost horizontal in the study area. More than 500 fault slip measurements from 41 different sites in the Tuzgölü basin were collected. For each reading, fault plane attitude, the orientation of slickenline and movement sense and relative dating markers were measured in the field. Cross-cutting relationships of slickenlines (if exist) were noted. Moreover, displaced stratigraphy along the faults was recorded in the field to estimate the slip timings.

Paleostress Analyses

Fault plane and fault lineation data collected from the field were analyzed by using T-Tecto software (Zalohar and Vrabec, 2007). This software is suitable for grouping deformation phases belonging to sedimentary basins in which dominant fault planes are measured from different lithologies allowing faults to act as heterogeneous structures because the software works based on the Gauss method (Zalohar and Vrabec, 2007). Pre-defined values and restrictions of the software are given in the study mentioned above. Meanings of relevant parameters are also summarized in an article (Gülyüz et al., 2019) similar to this study.

Basically, paleostress analyses aim to define principle stress directions prevailed in a region and it is based on four assumptions (Bott, 1959; Wallace, 1951; Angelier, 1984, 1989,1994; Armijo et al., 1982; Carey-Gailhardis and Mercier, 1987; Etchecopar et al., 1981; Fleischmann and Nemcok, 1991; Reches, 1987; Will and Powell, 1991); (i) faulted rock volume is homogeneous and isotropic, (ii) ductile deformations and rotations are not observed on fault planes, (iii) rock volume is faulted under spatio-temporally stable stresses and (iv) maximum shear direction is the same with the movement vector determined on fault plane and movement along a fault plane is independent of the other faults that are active during same deformation phase. Also, reliable paleostress analyses based on multi-measurements from different fault planes are directly related to age control of faulting activities, however during data collection determining age control parameters is not always possible due to occasional lack of suitable outcrops. In this respect, paleostress solutions without age control are grouped by considering similar paleostress solutions with age controls. In this study, such a grouping strategy was followed in order to determine the different deformation phases of the region. In addition to this strategy, a numeric index (Φ') determined by Delvaux et al. (1997) was also considered during the grouping of paleostress solutions. The index is basically depending on the shape factor of paleostress ellipsoids ($\Phi = (\sigma2-\sigma3)/(\sigma1-\sigma3)$) and formulated in 3 variant forms (i) $\Phi' = \Phi$ where σ1 close to vertical, (ii) $\Phi' = 2-\Phi$ where σ2 close to vertical and (iii) $\Phi' = 2 + \Phi$ where σ3 close to vertical. Also, tectonic settings are defined by considering the value of Φ' as; radial extensional ($0 < \Phi' < 0.25$), pure extensional ($0.25 < \Phi' < 0.75$), transtensional ($0.75 < \Phi' < 1.25$), pure strike-slip ($1.25 < \Phi' < 1.75$), transpressive ($1.75 < \Phi' < 2.25$), pure compressional ($2.25 < \Phi' < 2.75$) and radial compressional ($2.75 < \Phi' < 3$).

RESULTS

3.1 Structures in the basin

The tectonic evolution of the Tuzgölü Basin, based on stratigraphic development, is explained by two settings. These are defined as Neotethyan and post-Neotethyan settings, which are differentiated by an unconformity at the base of Eocene deposits. The former setting is represented pre-Oligocene marine sequences while the latter one is characterized by Oligocene to recent continental origin deposits. Similar to the stratigraphic analogy of the basin, structures in the region can also be grouped. In this regard, structures of the Neotethyan portion of the basin are mainly represented by almost NNW-SSE trending thrust faults and folds and the younger post-Neotethyan structures with similar trends are generally normal faults or strike-slip faults (Figure 2 and 3). Although the re-worked Tuzgölü Fault zone, one of the major active structures in the basin, is considered to be also a Neotethyan basin-bounding old fault in the region (Çemen et al., 1999) as discussed below, the well-preserved older (Neotethyan) structures within the basin infill are mainly observed as isolated outcrops and their extends are not long enough to map.

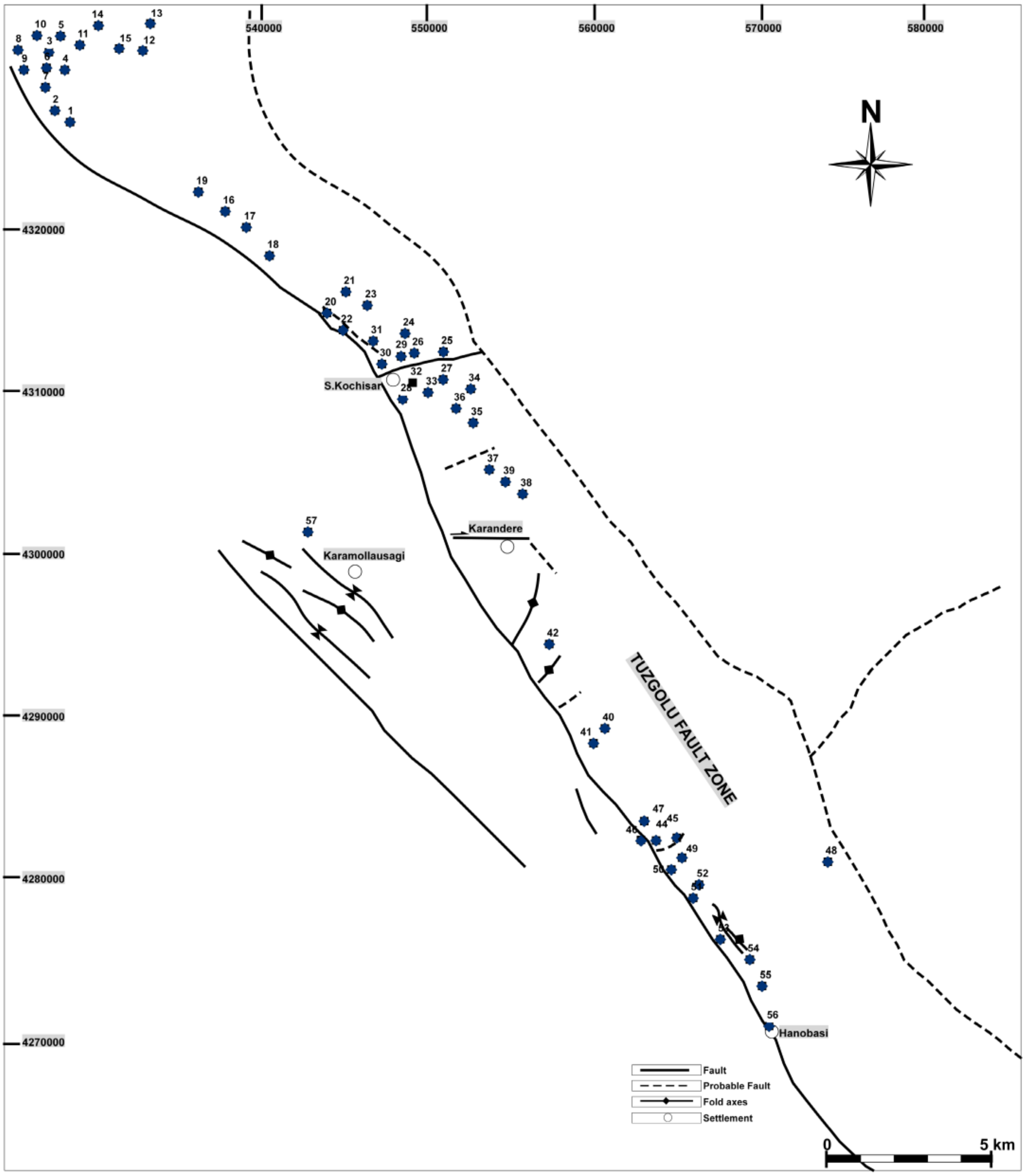

Figure 3. Major structures and paleostress measurement sites in the basin.

Şekil 3. Havzadaki temel yapılar ve paleostres ölçüm lokasyonları.

On the other hand, younger post-Neotethyan structures in the basin and surrounding areas are traceable in the field (Figure 1 and 2). The younger structures observed in the field can be considered as the components of the Tuzgölü Fault Zone while the other major structures at the west and south of the basin as Eskişehir, Sülüklü, and Akşehir fault zones are independent structures (Figure 1).

Although the structures in the basin are grouped in different settings, the line length rose diagrams of the Neogene/pre-Neogene structures (mainly folds) and bedding attitudes of pre-Neogene units are almost parallel to each other. According to the rose diagrams (Figure 2), the majority of the structures are characterized by almost NNE-SSW trends; however, there are also some secondary ENE-WSW trending structures.

Paleostress Inverse Solutions

From 41 fault plane measurement sites (10 of them with age control) around 500 slickenlines were noted and 57 paleostress inverse analyses were conducted by using these databases (Table 1 and Figure 3 and 4). Based on (Φ') index, 8 pure extension, 9 pure compression, 12 radial extension, 1 radial compression, 14 transpressive, 5 transtensive, 8 pure strike-slip stress orientations were determined. Paleostress inverse solution results are given in Table 1 and cyclographic traces, slickenlines and constructed paleostress configurations of the fault plane measurements are given in Figure 4. Also, photos of each fault plane measurement sites are given in Appendix A. Based on age controls and similar paleostress orientations, measurement sites were grouped in order to differentiate deformation phases in the region. In this regard, (i) 8 inverse solutions indicating almost E-W compressional setting by almost horizontal $\sigma1$ and vertical $\sigma3$, and 9 inverse solutions indicating almost N-S extensional setting by almost horizontal $\sigma3$ and vertical $\sigma1$ were grouped as the products of same deformation phase, (ii) 9 solutions showing NNW-SSE directed compression by almost horizontal $\sigma1$ and vertical $\sigma3$, 6 solutions indicating perpendicular extension direction were considered as solutions of the same group, (iii) 13 inverse solutions suggesting NW-SE transtensional setting by vertical $\sigma1$, almost horizontal $\sigma3$ and vertical to horizontal $\sigma2$ directions were attributed to the last deformation phase of the study area. The age control and stress orientation of the first group roughly indicate development almost N-S trending compressional faults and associatively formed E-W trending extensional faults during Late Cretaceous to Eocene time interval.

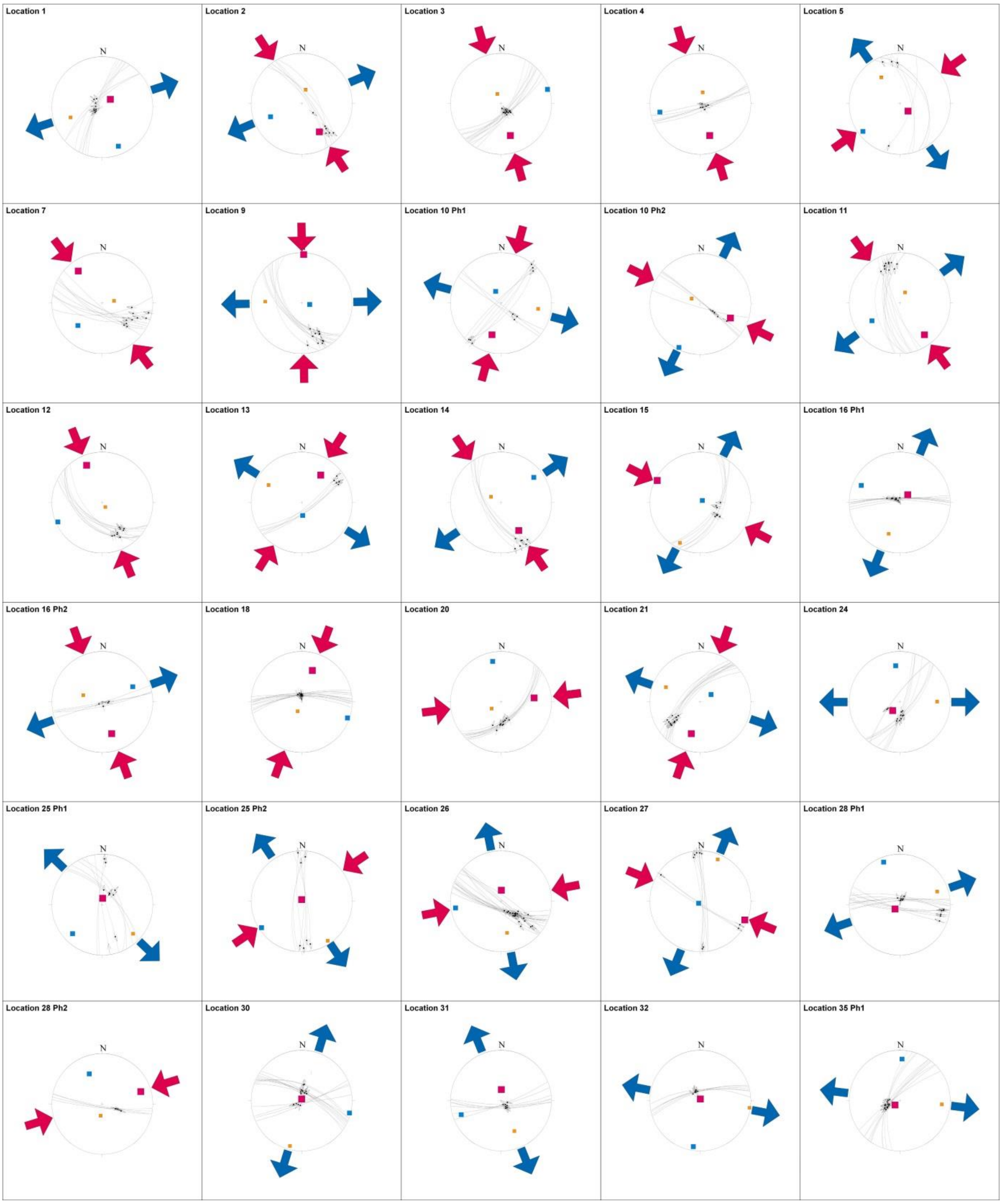

Figure 4. Cyclographic traces, slickenlines and paleostress configurations constructed with the Tuzgölü Basin fault plane measurements.

Şekil 4. Tuzgölü Havzası fay düzlemi ölçümlerinin stereonet üzerindeki izleri ve fay çiziklerine göre inşa edilmiş paleostress konfigürasyonları.

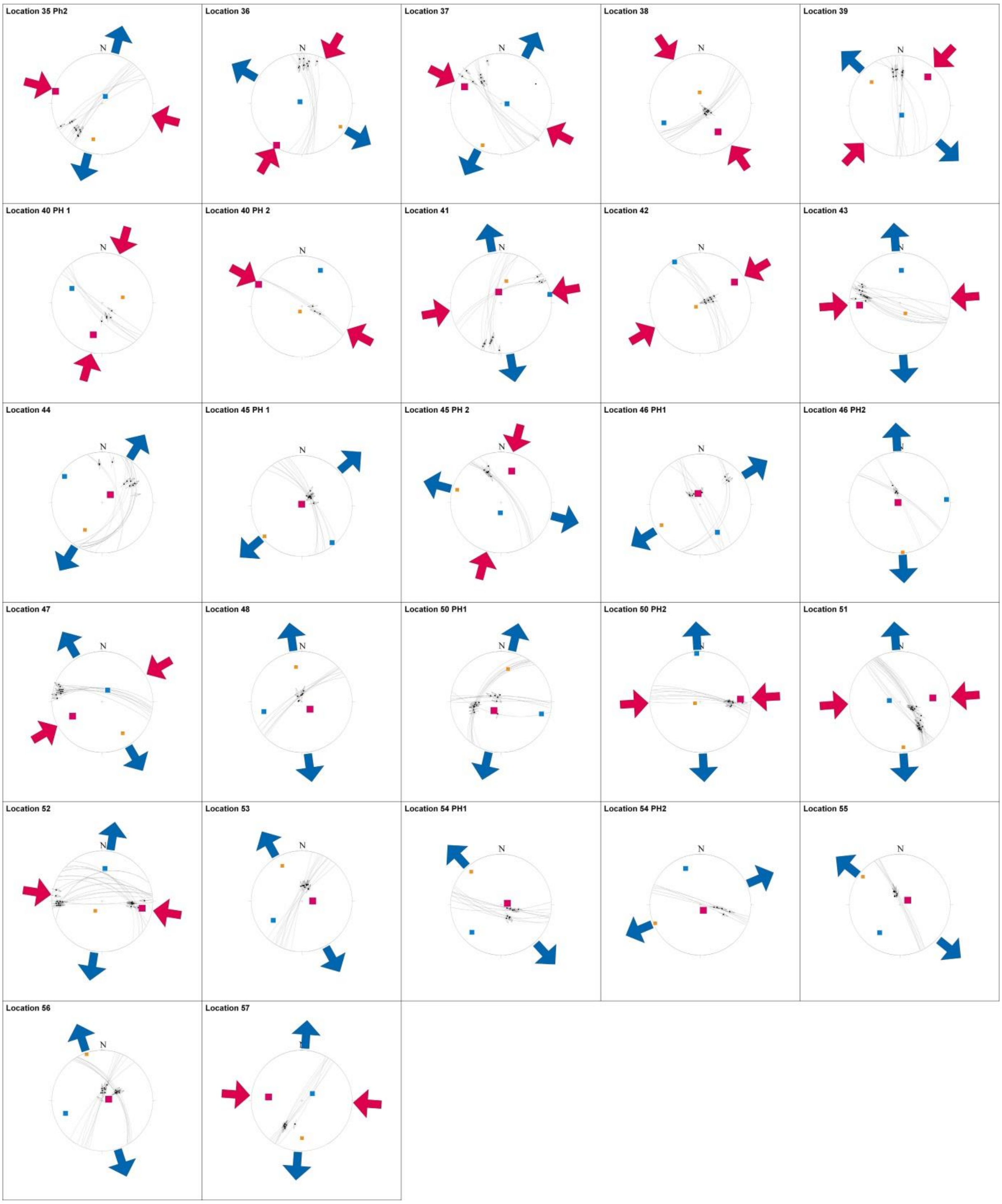

Figure 4. cont.

Şekil 4. Devamı.

The same kinematic analogy is also valid for the second group represented by ENE-WSW directed compressional and NNW-SSE directed extensional faults probably developed during Oligocene?-Pliocene time interval. The last group is represented by multi-directed extensional or transpressive faults. The age controls of the groups are given in Table 1 and their field photos are given as Appendix A. Also, contour diagrams of principal stress directions (σ1-2-3) of each group are given in Figure 5.

DISCUSSION

Neo-Tethyan Structural Development

Structural traces of the Neo-Tethys Ocean in the Central Anatolia are observed in Upper Cretaceous to Oligocene marine setting basins as Haymana, Çankırı, Tuzgölü, and Ulukışla basins. The structures in the Haymana and Çankırı basins elongate parallel to the İAESZ, while they follow the trend of ITSZ in the Tuzgölü and Ulukışla basins (Görür et al., 1984; Clark and Robertson, 2002; Kaymakcı et al., 2009; Gürer et al., 2018; Gülyüz et al., 2019) which implies independent developments of the basins along different branches of the ocean. In this regard, the Neo-Tethyan structures trend in NNW-SSE direction in the Tuzgölü Basin, but nevertheless the main Neo-Tethyan basin-bounding faults are not observed in the field due to the Neogene cover or effects of the overprinting deformation events in the region. However, some isolated intra-basinal fault outcrops and mappable folds within the Neotethyan marine units with almost NNW-SSE directed trends are found in the basin. Additionally, a major fault plane, the active Tuzgölü Fault, is explained as a basin bounding normal fault for the pre-Oligocene development of the basin by interpreting a low-quality seismic profile (Çemen et al., 1999). However, this interpretation is highly open to doubt and may lead to misunderstanding in the history of the Tuzgölü fault due to the degrees of detail and precision of some arguments evaluated in the study such as quality of the seismic data, which does not allow tracing of the units and structures older than Neogene and the absence of stratigraphic relations showing the differentiations in the direction of movement of the fault as diversification in thickness distribution or complex offset relationships along the fault plane. Except for this study, there is no another argument suggesting extension for the pre-Oligocene history of the Tuzgölü basin. However, similarities between the Tuzgölü and the Ulukışla Basins in terms of their tectonic positions, which is defined as being located between the Kırşehir Massif and Tauride Block, may allow correlating their deformation histories. In this respect, a limited number of studies suggesting extensional setting during Late Cretaceous-Paleocene time interval in the Ulukışla basin (Gautier et al., 2002; 2008; Gürer et al., 2018) might be considered as a supportive argument providing indirect evidence for the sole study (Çemen et al., 1999) suggesting extensional setting to the pre-

Oligocene period of the Tuzgölü Basin. However, findings of this study indicating almost E-W directed compression together with almost N-S directed extension for that time interval do not support an extension setting in the Tuzgölü basin for the relevant period. Although the results on existence of the pre-Oligocene extensional structures in the Tuzgölü basin (Çemen et al., 1999)

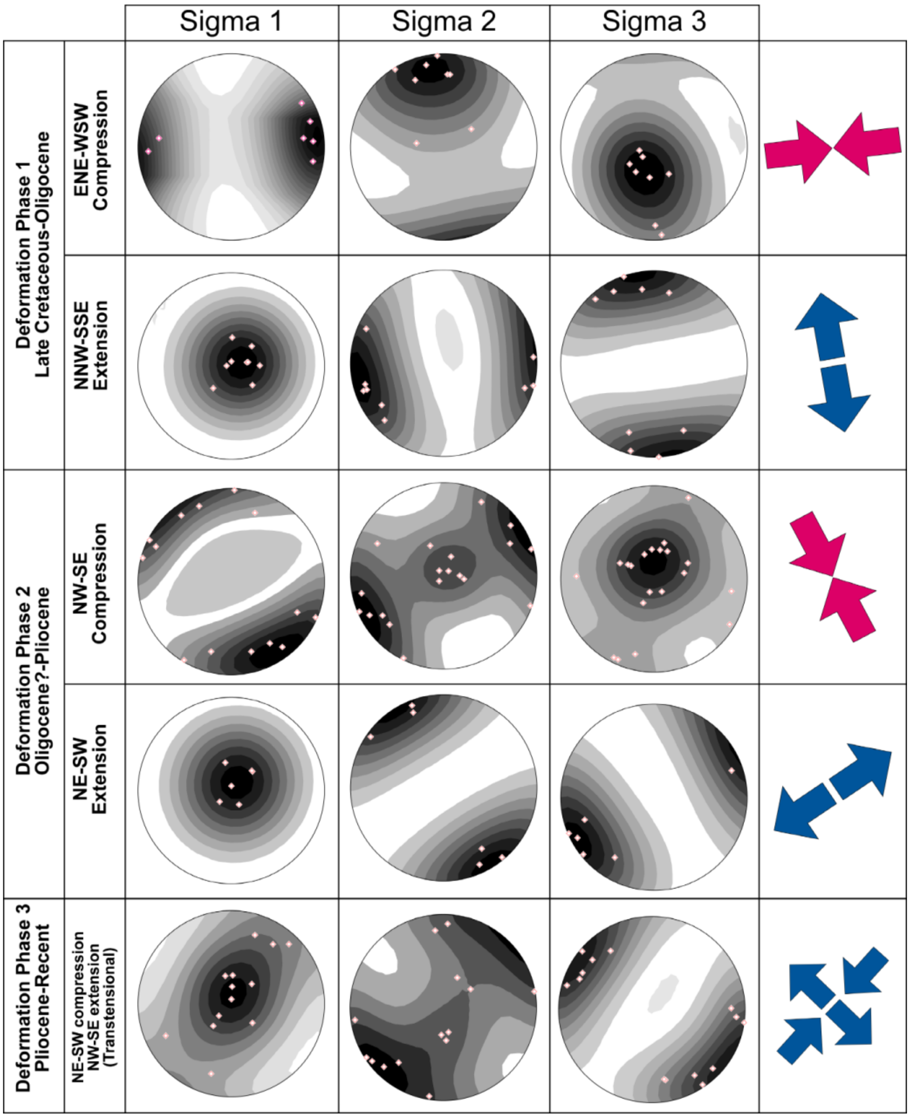

Figure 5. Deformation phases (phase 1, 2 and 3) based on paleostress inversion solutions. Contour diagrams of principle stress directions (sigma1-2-3) found after paleostress inversions. Each phase represents paleostress solutions coming from almost/probably same age (relatively dated) fault planes. Note that phases are represented by different type of faults and contour diagrams represent mean principle stress directions obtained from same types of faults. Each data point (black circles) represents principle stress direction of an individual paleostress inversion solution of a single paleostress location given in Table 1. Mean stress direction arrows represents a direction calculated from contour diagrams (stress direction of normal faults is the mean of sigma 3, stress direction of thrust/reverse

faults is the mean of sigma 1 and stress direction of strike-slip faults with reverse component is the mean of sigma 1 and 3.

Şekil 5. Paleostres ters çözümlerine dayalı deformasyon fazları (faz 1, 2 ve 3). Paleostress ters çözümlemelerinden sonra bulunan asal gerilme yönlerinin (sigma1-2-3) kontur diyagramları. Her faz, hemen hemen / muhtemelen aynı yaştaki (göreceli tarihlendirilmiş) fay düzlemlerinden gelen paleostres çözümlerini temsil eder. Fazlar farklı tipteki faylarla temsil edilirken kontur diyagramları aynı tip faylardan elde edilen ortalama temel gerilim yönlerini temsil etmektedir. Her veri noktası (siyah daireler), Tablo 1'de verilen tek bir paleostres konumundan elde edilen ayrı üç farklı temel gerilim yönünden birini temsil etmektedir. Ortalama gerilme yönü okları, kontur diyagramlarından hesaplanan bir yönü temsil etmektedir (normal fayların gerilme yönü sigma 3'ün ortalamasıdır bindirme / ters fayların gerilme yönü sigma 1'in ortalamasıdır ve ters bileşenli doğrultu atımlı fayların gerilme yönü sigma 1 ve 3'ün ortalamasıdır).

indicates similar deformation history with the Ulukışla basin, the NNW-SSE elongation of both the pre-Oligocene (Neo-Tethyan) basin infill and their compressional structures (folds and thrusts) shown in this study also suggest that the N-S directed extension in the Tuzgölü basin might be interpreted as the product of the main E-W-directed compressional setting in the region (Figure 5). On the other hand, compressional regime for the Central Anatolia in association with the closure of the Neo-Tethys Ocean is suggested in various studies (e.g. Görür et al., 1984; Kaymakcı et al., 2009; Gülyüz et al., 2013; Lefebvre et al., 2013; Gülyüz et al., 2019) for the pre-Oligocene. Briefly, these studies suggest that the Tertiary Central Anatolian basins started to form in fore-arc setting during Late Cretaceous in front of the Kırşehir or Pontide Block along the proto-ITSZ and İAESZ, respectively and latterly they were shortened due to progressive continental collision until Oligocene while the Ayhan-Büyükkışla basin, a basin located completely on the Kırşehir Block, was evolving under the effects of back-arc extensional to retro-arc foreland compressional settings (Advokaat et al., 2014). This scenario is suitable for the findings of this study which comprise the first direct field evidence indicating compressional setting for the Neo-Tethyan evolution of the basin. Since the time constraints of this study is based on the published fossil content of the units affected by the measured faults, the suggestions for the commencement and the end of the proposed regime are still blur. Therefore, age controls of the fault plane measurements should be enhanced by well-dated sequences in future studies.

Table 1. Locations and the results of paleostress analyses.

Çizelge 1. Paleostres analiz sonuçları ve analiz istasyonlarının konumları.

Location	Latitude	Logitude	Sigma 1	Sigma 2	Sigma 3	n	M°	Φ′	Φ′	Regime	Phase	Unit Age
1	39.18461	33.22143	48/65	155/10	252/23	9	8	0.4	0.4	Pure extension	Phase2	U.Mio-Pliocene
2	39.18518	33.22054	148/23	247/2	16/57	7	20	0.1	2.1	Transpressive	Phase2*	U.Mio-Pliocene
3	39.22325	33.22129	164/23	73/2	339/67	12	6	0.6	2.6	Pure compression	Phase2	Paleocene
4	39.22316	33.22182	164/23	258/11	12/64	6	10	0.5	2.5	Pure compression	Phase2	Paleocene
5	39.22328	33.22258	132/65	233/5	325/24	5	18	1	1	Transtensive	Phase3	Paleocene
7	39.20984	33.19952	323/12	228/23	79/63	10	20	0.3	2.3	Pure compression	Phase2*	U.Mio-Pliocene
9	39.20891	33.19874	2/2	99/72	272/18	11	11	0.1	1.9	Transpressive	Phase2*	Oligocene-L. Mio
10-PH1	39.23181	33.20845	196/23	336/61	99/17	9	16	0.2	1.8	Transpressive	Phase2	Paleocene
10-PH2	39.23181	33.20845	115/23	206/2	300/67	5	19	0.2	2.2	Transpressive	Phase2	Paleocene
11	39.22445	33.22629	142/12	237/23	26/63	11	10	0.2	2.2	Transpressive	Phase2*	Paleocene
12	39.24659	33.30156	337/13	247/2	148/77	9	8	0.3	2.3	Pure compression	Phase2	Paleocene
13	39.24754	33.30199	35/23	175/61	298/17	5	3	0.3	1.7	Pure strike-slip	Phase3	Paleocene
14	39.25347	33.28713	148/23	53/11	299/64	7	9	0.1	2.1	Transpressive	Phase2	Oligocene-L. Mio
15	39.25188	33.28947	297/2	45/84	207/6	7	8	0.2	1.8	Transpressive	Phase2	Oligocene-L. Mio
16-PH1	39.09593	33.39613	46/65	294/10	200/23	8	13	0.2	0.2	Radial extension	Phase1	Oligocene-L. Mio
16-PH2	39.09593	33.39613	164/23	64/22	295/57	4	8	0.2	2.2	Transpressive	Phase2	Oligocene-L. Mio
18	39.0926	33.39642	19/23	109/2	204/67	12	4	0.7	2.7	Pure compression	Phase2	Oligocene-L. Mio
20	39.05291	33.44837	83/23	348/11	235/64	10	17	0.8	2.8	radial compression	Phase1	Oligocene
21	39.05283	33.44853	196/23	56/61	293/17	11	9	0.3	1.7	Pure strike-slip	Phase3	Oligocene
24	38.96522	33.53564	219/65	354/18	89/16	11	16	0	0	Radial extension	Phase3*	Oligocene
25-PH1	38.97428	33.57467	3/75	225/11	134/10	9	16	0.4	0.4	Pure extension	Phase3	Oligocene
25-PH2	38.97428	33.57467	3/86	237/2	146/3	7	6	1	1	Transtensive	Phase3	Oligocene
26	38.958	33.55645	3/65	262/5	169/24	20	24	1	1	Transtensive	Phase3	L-M Eocene
27	38.95801	33.55693	113/2	221/84	23/6	10	11	0.7	1.3	Pure strike-slip	Phase2*	L-M Eocene
28-PH1	38.95824	33.55647	226/76	339/6	71/13	13	17	0.4	0.4	Pure extension	Phase2	L-M Eocene
28-PH2	38.95824	33.55647	72/12	337/23	188/63	4	5	0.6	2.6	Pure compression	Phase1	L-M Eocene
30	38.95614	33.55227	2/86	104/1	195/4	14	9	0.1	0.1	Radial extension	Phase1*	L-M Eocene
31	38.95655	33.55203	2/65	251/10	156/23	7	8	0.3	0.3	Pure extension	Phase1	L-M Eocene
32	38.95676	33.55184	2/86	189/4	98/0	6	5	0.1	0.1	Radial extension	Phase3	L-M Eocene
35-PH1	38.9213	33.6041	226/75	3/11	95/10	12	11	0.1	0.1	Radial extension	Phase3	Oligocene-L. Mio
35-PH2	38.9213	33.6041	285/2	21/72	194/18	10	7	0.8	1.2	Transtensive	Phase2	Oligocene-L. Mio
36	38.92739	33.59287	211/2	320/84	121/6	10	10	0	2	Transpressive	Phase2	Oligocene-L. Mio
37	38.89059	33.61722	295/12	89/76	204/6	10	26	0.1	1.9	Transpressive	Phase2	Oligocene-L. Mio
38	38.88671	33.61792	148/23	242/11	356/64	9	6	0.3	2.3	Pure compression	Phase2	Oligocene-L. Mio
39	38.89018	33.61977	44/12	168/68	310/18	11	8	0.6	1.4	Pure strike-slip	Phase3	Oligocene-L. Mio
40-PH1	38.7541	33.69154	196/23	296/22	65/57	6	6	0.4	2.4	Pure compression	Phase2	Oligocene-L. Mio
40-PH2	38.7541	33.69154	297/2	27/12	198/78	3	9	0.4	2.4	Pure compression	Phase2	Oligocene-L. Mio
41	38.74854	33.68666	348/65	80/1	170/25	11	14	0.9	0.9	Transtensive	Phase3	Oligocene-L. Mio
42	38.79656	33.65648	58/12	328/2	229/77	8	4	1	2.1	Transpressive	Phase1	Paleocene
43	38.79656	33.65648	267/12	3/23	151/63	11	8	0	2	Transpressive	Phase1	L-M Eocene
44	38.70239	33.72344	46/65	305/5	213/24	10	20	0.5	0.5	Pure extension	Phase2	L-M Eocene
45-PH1	38.70238	33.72325	2/86	140/3	231/3	10	14	0.2	0.2	Radial extension	Phase2	L-M Eocene
45-PH2	38.70238	33.72325	19/23	184/66	286/6	7	8	0.4	1.6	Pure strike-slip	Phase3	L-M Eocene
46-PH1	38.70242	33.72306	348/65	148/24	242/8	10	20	0.1	0.1	Radial extension	Phase2	L-M Eocene
46-PH2	38.70242	33.72306	273/86	86/4	177/0	5	10	0.2	0.2	Radial extension	Phase1	L-M Eocene
47	38.70486	33.73149	244/23	25/61	147/17	10	5	0.4	1.6	Pure strike-slip	Phase3	Eocene
48	38.7577	33.79009	132/65	255/14	351/20	7	9	0.1	0.1	Radial extension	Phase1	U.Mio-Pliocene
50-PH1	38.68651	33.73611	219/65	107/10	12/23	15	13	0.1	0.1	Radial extension	Phase1	U. Senonian
50-PH2	38.68651	33.73611	86/13	356/2	257/77	8	4	0.1	2.1	Transpressive	Phase1	U. Senonian
51	38.6525	33.76335	83/23	278/66	175/6	20	28	0.3	1.7	Pure strike-slip	Phase1*	Paleocene
52	38.65086	33.76217	100/12	5/23	216/63	18	12	0.1	2.1	Transpressive	Phase1	U. Senonian
53	38.62219	33.78893	89/65	236/21	331/12	11	6	0.4	0.4	Pure extension	Phase1	Paleocene
54-PH1	38.5811	33.81594	77/75	226/13	318/7	9	13	0.1	0.1	Radial extension	Phase1	L-M Eocene
54-PH2	38.5811	33.81594	151/76	338/14	247/1	5	16	0.3	0.3	Pure extension	Phase2	L-M Eocene
55	38.56832	33.8173	46/65	219/25	310/3	8	9	0.3	0.3	Pure extension	Phase3	Eocene
56	38.56486	33.8224	77/76	251/14	341/1	15	19	0.1	0.1	Radial extension	Phase1	Eocene
57	38.84338	33.49276	277/23	57/61	179/17	8	15	0.7	1.3	Pure strike-slip	Phase1	L-M Eocene

Φ stress ratio, Φ′ Numeric index of Delvaux et al. (1997), n: number of samples, M° maximum misfit angle between trends of actual and calculated slickenlines.

Post-Neo-Tethyan Structural Development

Termination of the Neo-Tethys Ocean in the region is marked by a regional unconformity at the base of Oligocene continental deposits (Kaymakcı et al., 2001; Koçyigit, 1991; Şengör et al., 1985) which can also be considered as the commencement of the on-going continental deposition in the Central Anatolia. The first deposits of this phase are mainly represented by evaporates and coal-bearing swamp environment deposits (Arıkan, 1975; Derman, 1978; Dellaloğlu and Aksu, 1984; Görür et al., 1984; Çemen et al., 1999). This point out a close basin probably developed after the complete closure of the ocean. Deformation markers of this term in the Central Anatolia are characterized by strike-slip or reverse faults developed because of the further convergence after the continental collision event (Kaymakcı et al., 2001; Kaymakcı et al., 2009; Genç and Yürür 2010; Gülyüz et al., 2013; Gülyüz et al., 2019). The main structures of the phase in the region are the re-worked Dereköy strike-slip fault in the Haymana Basin and Hirfanlar-Hacıbektaş, Delice Kozaklı and Savcılı fault zones located directly on the Kırşehir Block (Lefebvre et al., 2013; Özkaptan and Gülyüz, 2019; Gülyüz et al., 2019). Although there is no defined major structure in the Tuzgölü basin for that term, isolated small-scale (<500m) fault planes sealed by Pliocene deposits are common in the basin. Paleostress inverse solutions of these fault planes are represented by NNW-SSE-directed compressional and ENE-WSW-directed extensional principal stress directions. Such paleostress inverse solutions are not consistent with the possible further convergence direction of the Tauride Block with respect to the Kırşehir Block. However, almost N-S-directed regional compressional regime observed in the Central Anatolia related to further convergence between the Pontide Block and Tauride-Anatolide Block including the Kırşehir block (e.g. Kaymakcı et al., 2001; 2009) might be attributed the NNW-SSE directed compressional regime defined in this study. On the other hand, the stress regime of this phase may also be attributed to the segmentation of the Kırşehir Block after its indentation into the Pontide Block during the continental collision along the İAESZ. The timing of the segmentation is blur due to the evidence coming from paleomagnetic rotations of central Anatolian Granitoids with late Cretaceous-Paleocene emplacement ages (Lefebvre et al., 2013) and suggesting only post-Paleocene age for the segmentation. The results presented in this study may give a time constraint for the segmentation event by indicating NNW-SSE-directed compressional setting, which is also suggested in the segmentation model of the related study (Lefebvre et al., 2013). Although Lefebvre et al. (2013) suggest that the segmentation of the defined block occurred during the indentation event (non-rigid indenter model), the segmentation might be occur after completion of the indentation history due to the nature of the indenting mass that should be solid enough to not yet break during the indentation event. In this regard, the segmentation of the Kırşehir block should have occurred after the continental collision (indentation) event. This seems more appropriate in comparison with the syn-indentation model proposed by Lefebvre et al (2013). In addition, segmentation of the KB may be linked to the strain accommodation within the block itself after the complete indentation of the block. Although the results in the study do not sufficiently give a time limit for the end of this deformation phase, the results presented in Özsayın et al. (2013) with radiogenic ages suggesting pre ~ 6 Ma might be considered as the termination of the phase Additionally, it also can be considered that the deformation in the region for that time interval might be enhanced by the effect of two dynamic factors as (i) the escape tectonic due to the continental collision between the Eurasian and Arabian Plates in south-eastern Turkey and (ii) pulling due to Aegean subduction system. However, our results do not fit these models, which may have created trans-tensional regime in the region. This inconsistency may be explained by the dominant effect of the almost N-S directed convergence events going on up to ~6 Ma in the region.

Neotectonic Structural Development

The northward movement of Arabian Plate in the east and pull effect of Aegean subduction systems in the west are the main driving force behind the neotectonic deformation in the Anatolian Plate. The Central Anatolian Plateau is located at the transition zone of these main deformational forces. Additionally, remnants of older Neotethyan and younger Mediterranean/Aegean subduction systems below the Plateau resulted in >1 km uplift of the entire plateau by arc-root removal (drip tectonics) or slab-break off Mediterranean/Aegean slabs (Göğüş et al. 2017; Schildgen et al., 2012; 2014). The kinematic traces of these events in the Tuzgölü Basin and in the Central Anatolia are discussed in various studies (e.g. Aydar et al., 2013; Schildgen et al., 2012; 2014; Çiner et al., 2015; Özsayın et al., 2013; Yıldırım et al., 2016; Çubuk et al., 2014). The one presenting data directly from the Tuzgölü Basin, Özsayın et al. (2013), suggests extensional tectonics since ~6 Ma for the basin. Although the age constraints of the last phase defined in this study do not give robust evidence for the commencement of the regime, 6,81 Ma age (Özsayın et al., 2013) might be considered as the commencement of the phase due to the paleostress inversion solutions showing a similar character with the previous study as being dominantly resulted from extensional structures with some dextral component. On the other hand, the rapid uplift of the Central Anatolia is associated with the drip tectonic model since ~10 Ma and this suggestion is not fully supported by 6,81 Ma and younger extensional tectonics in the region. The 6,81 Ma age of Özsayın et al. (2013) is based on dating an ignimbrite unit laying on red fluvial clastics which covers an angular unconformity representing contractional to extensional regime transitions in the basin. This implies that the actual commencement age of the phase must be older than the proposed age because of the unknown depositional time interval of the red clastics. Therefore, ~10 Ma seems a more plausible age for the commencement of the last phase.

The commencement of the lithospheric drip at ~10 Ma and associated extensional tectonic is explained by the asthenospheric mantle entrainment under the Anatolian plate from the east (Göğüş et al., 2017). Additionally, a slab window under Cyprus since ~2 Ma is considered as the secondary effect on the uplift of the region (Göğüş et al., 2017). The results presented in this study indicate that such an uplift history might be controlled by normal Tuzgölü Fault zone with minor dextral component along the western margin of the plateau. However, the results do not allow differentiating slab window effect from the drip tectonics due to limitations in dating fault plane measurements.

CONCLUSIONS

- The Tuzgölü Basin has structural records of Neotethyan and post-Neotethyan development of the Central Anatolia.

- Fault planes related to the Neotethyan development of the basin do not present large traces, while some NNW-SSE-trending folds are traceable in the basin. On the other hand, small scale isolated fault planes are frequently observed within the Upper Cretaceous to Oligocene deposits.

- Late Cretaceous to recent structural development of the basin is represented by three different deformation phases.

- The first phase is represented by almost E-W directed compressional and coevally developed almost N-S directed extensional principal stress directions. This phase is attributed to the fore-arc to foreland stages of the Tuzgolü basin in association with the closure of a Neotethyan branch along the almost N-S directed ITSZ during Late Cretaceous to Oligocene time interval.

- The second phase is represented by NNW-SSE-directed compressional and coevally developed ENE-WSW directed extensional principal stress directions. This phase comprises the segmentation of the Kırşhehir block after its indentation into the Pontide block along the İAESZ due to the further northward movement of the Tauride-Anatolide and possibly Africa plates during Oligocene to Pliocene time interval.

• The last phase is represented by a transtensional regime with almost vertical sigma 1 and NW-SE directed almost horizontal sigma 3 directions. The regional uplift of the Central Anatolian Plateau is considered as the reason behind the deformation phase.

• The principal stress directions presented in this study are independent from possible vertical block rotations, therefore results of future paleomagnetic studies are needed for presenting more precise stress direction results.

ACKNOWLEDGEMENTS

This study was supported by the Scientific and Technical Research Council of Turkey (TÜBİTAK, 117R049) for field works. The study benefited from discussions with Nuretdin Kaymakcı and Nilay Gülyüz.

REFERENCES

Advokaat, E.L., van Hinsbergen, D.D.J., Kaymakcı, N., Vissers, R.L.M. , Hendriks, B.W.H., 2014. Late Cretaceous extension and Palaeogene rotation related contraction in Central Anatolia recorded in the Ayhan-Büyükkışla basin, International Geology Review, 56, 1813-1836.

Akarsu, İ., 1971. II. Bölge AR/TPO/747 nolu sahanın terk raporu. Pet. İş. Gen. Md., Ankara (Unpublished).

Angelier, J., 1984. Tectonic analysis of fault slip data sets. Journal of Geophysical Research, 89, 5835-5848.

Angelier, J., 1989. From orientation to magnitudes in paleostress determinations using fault slip data. Journal of Structural Geology, 11, 37-50.

Angelier, J., 1994. Fault slip analysis and paleostress reconstruction. In: P.L. Hancock (Editor), Continental deformation. Pergamon Press, Oxford, 53-101.

Arikan, Y., 1975. The Geology and Petroleum prospects of the Tuzgölü basin, Maden Tektik ve Arama Dergisi, 85, 17-38.

Armijo, R., Carey, E., Cisternas, A., 1982. The inverse problem in microtectonics and the separation of tectonic phases. Tectonophysics, 82, 145-160.

Aydar, E., Cubukcu, H.E., Şen, E., Akın, L., 2013. Central Anatolian Plateau, Turkey: incision and paleoaltimetry recorded from volcanic rocks. Turkish J. Earth Sci. 22, 739–746.

Aydemir, A., Ates, A., 2006. Structural interpretation of the Tuzgolu and Haymana Basins, Central Anatolia, Turkey, using seismic, gravity and aereomagnetic data. Earth, Planets and Space, 58, 951–961.

Biryol, C. B., Beck, S., Zandt, G., Özacar, A. A., 2011. Segmented African lithosphere beneath the Anatolian region inferred from teleseismic P-wave tomography. Geophys. J. Int. 184, 1037–1057.

Bott, M.H.P., 1959. The Mechanics of Oblique Slip Faulting. Geol. Mag. 96, 109–117.

Burke, K., Şengör, A.M.C., 1986. Tectonic escape in the evolution of the continental crust. Reflect. Seismol. Cont. crust 14, 41–53.

Carey-Gailhardis, E., Mercier, J.L., 1987. A numerical method for determining the state of stress using focal mechanisms of earthquake populations: application to Tibetan teleseisms and microseismicity of Southern Peru. Earth Planet. Sci. Lett. 82, 165–179. https://doi.org/10.1016/0012-821X(87)90117-8

Candan, O., Cetinkaplan, M., Oberhänsli, R., Rimmele, G., Akal, C., 2005. Alpine high Pressure low-Temperature metamorphism of the Afyon Zone and implications for the metamorphic evolution of Western Anatolia, Turkey, Lithos 84(1-2), 102-124.

Çelik, Ö. F., Marzoli, A., Marschik, R., Chiaradia, M., Neubauer, F., Öz, I., 2011. Early–Middle Jurassic intra-oceanic subduction in the Izmir-Ankara-Erzincan Ocean, Northern Turkey, Tectonophysics, 509, 120–134.

Çemen, İ., Göncüoğlu, M.C., Dirik, K., 1999. Structural evolution of the Tuzgölü Basin in Central Anatolia, Turkey, Journal of Geology, 107, 693–706.

Çiner, A., Doğan, U., Yıldırım, C., Akçar, N., Ivy-Ochs, S., Alfimov, V., Kubik, P.W., Schlüchter, C., 2015. Quaternary uplift rates of the Central Anatolian Plateau, Turkey: insights from cosmogenic isochron-burial nuclide dating of the Kızılırmak River terraces, Quaternary Science Reviews.Volume 107,81-97.

Çinku, M.C., 2017. Paleomagnetic results from Northeast Anatolia: remagnetization in Late Cretaceous sandstones and tectonic rotation at the Eastern extension of the Izmir–Ankara–Erzincan suture zone. Acta Geophys. https://doi.org/10.1007/s11600-017-0097-7.

Çinku, M.C., Hisarli, M., Hirt, A.M., Heller, F., Ustaömer, T., Kaya, N., Öksüm, E., Orbay, N., 2016. Evidence of Late Cretaceous oroclinal bending in north-central Anatolia: palaeomagnetic results from Mesozoic and Cenozoic rocks along the İzmir–Ankara–Erzincan Suture Zone. Geol. Soc. London, Spec. Publ. 425, 189 LP – 212.

Çubuk, Y., Yolsal-Çevikbilen, S.,Taymaz, T., 2014. Source parameters of the 2005–2008 Balâ–Sırapınar (Central Turkey) earthquakes: implications for the internal deformation of the Anatolian plate. Tectonophysics 635, 125–153.

Clark, M., Robertson, A., 2002. The role of the Early Tertiary Ulukışla Basin, southern Turkey, in suturing of the Mesozoic Tethys Ocean, Journal of the Geological Society, 159(6), 673-690.

Dellaloğlu, A.A., Aksu, R., 1984. Polatlı, Haymana, Yenice, Yeniceoba ve Cihanbeyli dolaylarının Ayrıntılı Jeoloji ön raporu. TPAO rapor no.2006 (unpublished).

Delvaux, D., Moeys, R., Stapel, G., Petit, C., Levi, K., Miroshenko, A., Ruzhich, V., Sankov, V., 1997. Paleostress reconstructions and geodynamics of the Baikal region, Central Asia, Part 2. Cenozoic rifting. Tectonophysics, 282, 1–38.

Derman, A.S., 1978. Tuzgölü ve Kuzeyinin Jeolojisi. TPAO rapor no 1512 (unpublished).

Dirik, K., Erol, O., 2003. Tuzgölü ve civarının tektonomorfolojik evrimi, Orta Anadolu-Türkiye, TPJD Özel sayı, 27-46.

Erdoğan, B., Akay, E., Uğur, M.S., 1996. Geology of the Yozgat region and evolution of the collisional Çankiri Basin, International Geology Review, 38, 788-806.

Erler, A., Akıman, O., Unan, C., Dalkılıç, F., Dalkılıç, B., Geven, A., Önen, P., 1991. Kaman (Kırşehir) ve Yozgat yörelerinde Kırşehir masifi magmatik kayaçlarının petrolojisi ve jeokimyası, TÜBITAK, Doga-Tr. J. of Eng. and Env. Sc., 15, 76-100.

Erler, A., Göncüoglu, M.C., 1996. Geologic and tectonic setting of the Yozgat batholith, Northern Central Anatolian Crystalline Complex, Turkey, International Geology Review, 38 (8), 714-726.

Etchecopar, A., Vasseur, G., Daigniers, M., 1981. An inverse problem in microtectonics for the determination of stress tensors from fault striation analysis. Journal of Structural Geology, 3, 51-65.

Fernandez-Blanco, D., Bertotti, G., Çiner, T.A., 2013. Cenozoic tectonics of the Tuzgölü basin (Central Anatolian Plateau, Turkey). Turkish Journal of Earth Science, 22, 715-738.

Fleischmann, K.H., Nemcok, M., 1991. Paleostress inversion of fault-slip data using the shear stress solution of Means (1989). Tectonophysics 196, 195–202. https://doi.org/10.1016/0040-1951(91)90296-5

Flerit, F., Armijo, R., King, G., Meyer, B., 2004. The mechanical interaction between the propagating North Anatolian Fault and the back-arc extension in the Aegean. Earth Planet. Sci. Lett. 224, 347–362.

Gautier, P., Bozkurt, E., Hallot, E., Dirik, K., 2002. Dating the exhumation of a metamorphic dome: geological evidence for pre-Eocene unroofing of the Niğde Massif (Central Anatolia, Turkey), Geological Magazine, 139(5), 559-576.

Gautier, P., Bozkurt, E., Bosse, V., Hallot, E., Dirik, K., 2008. Coeval extensional shearing and lateral underflow during Late Cretaceous core complex development in the Niğde Massif, Central Anatolia, Turkey, Tectonics, 27, TC1003

Genç, Y., Yürür, M.T., 2010. Coeval extension and compression in Late Mesozoic-Recent thin-skinned extensional tectonics in central Anatolia, Turkey, Journal of Structural Geology 32(5), 623-640.

Göğüş, O.H., Pysklywec, R.N., Şengör, A.M.C., Gün, E., 2017. Drip Tectonics and the enigmatic uplift of the Central Anatolian Plateau. Nature Communications. 8. 10.1038/s41467-017-01611-3.

Göncüoğlu, M.C.,1986. Orta Anadolu Masifinin güney ucundan jeokronolojik yaş bulguları, MTA Bülteni, 105/106, 111-124.

Gürer, D., Plunder, A., Kirst, F., Corfu, F., Schmid, S., van Hinsbergen, D.W.W., 2018. A long-lived Late Cretaceous–early Eocene extensional province in Anatolia? Structural evidence from the Ivriz Detachment, southern central Turkey. Earth and Planetary Science Letters. 481. 10.1016/j.epsl.2017.10.008.

Görür, N., Oktay, F.Y., Seymen, I., Şengör, A.M.C., 1984. Palaeotectonic evolution of the Tuzgölü basin complex, Central Turkey: sedimentary record of a Neo-Tethyan closure, Journal of the Geological Society of London Special Publications, 17(1), 467-482.

Görür, N., Tüysüz, O., Şengör, A.M.C., 1998. Tectonic Evolution of the Central Anatolian Basins, International Geology Review, 40, 831-850.

Gülyüz, E., Kaymakci, N., Meijers, M.J.M., van Hinsbergen, D. J.J., Lefebvre, C.J.C., Vissers, R.L.M., Hendriks, B.W.H., Peynircioğlu, A.A., 2013. Late Eocene evolution of the Çiçekdağı Basin (central Turkey): Syn-sedimentary compression during microcontinent–continent collision in central Anatolia, Tectonophysics, 602, 286–299.

Gülyüz, E., Özkaptan, M., Kaymakci, N., Persano, C., Stuart, F.M., 2019. Kinematic and thermal evolution of the Haymana Basin, a fore-arc to foreland basin in Central Anatolia (Turkey). Tectonophysics. https://doi.org/10.1016/j.tecto.2019.06.020.

Gülyüz, E., Durak, H., Özkaptan, M., Krijgsman, W., 2020. Paleomagnetic constraints on the early Miocene closure of the southern Neo-Tethys (Van region; East Anatolia): Inferences for the timing of Eurasia-Arabia collision. Glob. Planet. Change 185, 103089.

Gürsoy, H., Piper, J.D.A., Tatar, O., 2003. Neotectonic deformation in the western sector of tectonic escape in Anatolia: Palaeomagnetic study of the Afyon region, central Turkey. Tectonophysics 374, 57–79. https://doi.org/10.1016/S0040-1951(03)00346-9

Gürsoy, Halil, Piper, J.D.A., Tatar, O., 1999. Palaeomagnetic study of the Galatean Volcanic Province, north-central Turkey: Neogene deformation at the northern border of the Anatolian Block. Geol. J. 34, 7–23. https://doi.org/10.1002/(SICI)1099-1034(199901/06)34:1/2<7::AID-GJ812>3.0.CO;2-0

Gürsoy, H., Piper, J.D.A., Tatar, O., Mesci, L., 1998. Palaeomagnetic study of the Karaman and Karapinar volcanic complexes, central Turkey: Neotectonic rotation in the south-central sector of the Anatolian Block. Tectonophysics 299, 191–211. https://doi.org/10.1016/S0040-1951(98)00205-4

Gürsoy, H., Tatar, O., Piper, J.D.A., Koçbulut, F., Akpinar, Z., Huang, B., Roberts, A.P., Mesci, B.L., 2011. Palaeomagnetic study of the Kepezdaĝ and Yamadaĝ volcanic complexes, central Turkey: Neogene tectonic escape and block definition in the central-east Anatolides. J. Geodyn. 51, 308–326. https://doi.org/10.1016/j.jog.2010.07.004

Hisarlı, Z.M., Çinku, M.C., Ustaömer, T., Keskin, M., Orbay, N., 2016. Neotectonic deformation in the Eurasia–Arabia collision zone, the East Anatolian Plateau, E Turkey: evidence from palaeomagnetic study of Neogene–Quaternary volcanic rocks. Int. J. Earth Sci. https://doi.org/10.1007/s00531-015-1245-4

Hüsing, S.K., Zachariasse, W.J., van Hinsbergen, D.J.J., Krijgsman, W., Inceöz, M., Harzhauser, M., Mandic, O., Kroh, A., 2009. Oligo-Miocene foreland basin evolution in SE Anatolia: constraints on the closure of the eastern Tethys gateway, in: van Hinsbergen, D.J.J., Edwards, M.A., Govers, R. (Eds.), Geodynamics of Collision and Collapse at the Africa-Arabia-Eurasia Subduction Zone: Geological Society, London, Special Publication. pp. 107–132.

Kadıoğlu, Y.K., Dilek, Y., Foland, K.A., 2006. Slab break-off and syn-collisional origin of the Late Cretaceous magmatism in the Central Anatolian crystalline complex, Turkey, Geological Society of America Special Paper, 409, 381–415.

Kaygusuz, A., Aydınçakır, E., 2009. Mineralogy, whole-rock and Sr-Nd isotope geochemistry of mafic microgranular enclaves in Cretaceous Dagbaşı granitoids, eastern Pontides, NE Turkey: evidence of magma mixing, mingling and chemical equilibration, Chemie der Erde, 69, 247-277.

Kaygusuz, A., Sipahi, F., İlbeyli, N., Arslan, M., Chen, B., Aydınçakır, E., 2013. Petrogenesis of the Late Cretaceous Turnagöl intrusion in the eastern Pontides: implications for magma genesis in the arc setting. Geoscience Frontiers, 4, 423–438.

Kaymakcı, N., Özçelik, Y., White, H.S., Van Dijk, P.M., 2001. Neogene tectonic development of the Çankırı basin (Central Anatolia, Türkiye). Turkish Assoc. Pet. Geol. Bull. 13, 27–56.

Kaymakcı, N., Duermeijer, C.E., Langereis, C., White, S.H., Van Dijk, P.M., 2003. Palaeomagnetic evolution of the Çankiri Basin (central Anatolia, Turkey): Implications for oroclinal bending due to indentation. Geol. Mag. https://doi.org/10.1017/S001675680300757X

Kaymakci, N., Özçelik, Y., White, S.H., Van Dijk, P.M., 2009. Tectono-stratigraphy of the Çankiri Basin: late Cretaceous to early Miocene evolution of the Neotethyan suture zone in Turkey, Journal of the Geological Society of London Special Publications, 311, 67-106.

Kaymakci, N., 2000. Tectono-stratigraphical evolution of the Cankiri Basin (Central Anatolia, Turkey), Geologica Ultraiectina, Phd. Thesis,190.

Kissel, C., Averbuch, O., Frizon de Lamotte, D., Monod, O., Allerton, S., 1993. First paleomagnetic evidence for a post-Eocene clockwise rotation of the Western Taurides thrust belt east of the Isparta reentrant (Southwestern Turkey). Earth Planet. Sci. Lett. 117, 1–14.

Kissel, C., Laj, C., Sengör, A.M.C., Poisson, A., 1987. Paleomagnetic evidence for rotation in opposite senses of adjacent blocks in northeastern Aegean and western Anatolia. Geophys. Res. Lett. 14, 907–910.

Le Pichon, X., Angelier, J., 1979. The Hellenic arc and trench system: a key to the neotectonic evolution of the Eastern Mediterranean area. Tectonophysics 60, 1–42.

Koçyiğit, A., Winchester, J.A., Bozkurt, E., Holland, G., 2003. Saraçköy Volcanic Suite: implications for the subductional phase of arc evolution in the Galatean Arc Complex, Ankara-Turkey, Geological Journal, 37, 1−14.

Koçyiğit, A., 1991. An example of an accretionary forearc basin from Central Anatolia and its implications for the history of subduction of Neo-Tethys in Turkey, Geological Society of America Bulletin, 103, 22-36.

Lefebvre, C.J.C., Meijers, M.J.M., Kaymakcı, N., Peynircioğlu, A.A., Langereis, C.G., Van Hinsbergen, D.J.J., 2013. Reconstructing the geometry of central Anatolia during the late Cretaceous: Large-scale Cenozoic rotations and deformation between the Pontides and Taurides, Earth and Planetary Science Letters, 366, 83-98.

Nairn, S.P., Robertson, A.H.F., Ünlügenç, U.C., İnan, N., Taslı, K., 2013. Tectonostratigraphic evolution of the Upper Cretaceous-Cenozoic central Anatolian basins: an integrated model of diachronous ocean basin closure and continental collision. Journal of the Geological Society of London Special Publication, 372, 343–384.

Okay, A.I., Sunal, G., Sherlock, S., Altıner, D., Tüysüz, O., Kylander-Clark, A.R.C., Aygül, M., 2013. Early Cretaceous sedimentation and orogeny on the southern active margin of Eurasia: Central Pontides, Turkey, Tectonics, 32, 1247–1271.

Okay, A. I., Tansel, I., Tüysüz, O., 2001. Obduction, subduction and collision as reflected in the Upper Cretaceous–Lower Eocene sedimentary record of western Turkey, Geological Magazine, 138, 117-142.

Okay, A.I., 1984. Distribution and characteristics of the northwest Turkish blueschists, Journal of the Geological Society of London Special Publications, 17, 455-466.

Okay, A., Altiner, D., Kylander-Clark, A., 2019. Major Late Cretaceous mass flows in central Turkey recording the disruption of the Mesozoic Continental Margin. Tectonics. https://doi.org/10.1029/2018TC005076

Özkaptan, M., Gülyüz, E., 2019. Relationship between the anisotropy of magnetic susceptibility and development of the Haymana Anticline, Central Anatolia (Turkey). Turkish J. Earth Sci. 28, 103–121.

Özsayın, E., Çiner, T.A., Rojay, F.B., Dirik, R.K., Melnick, D., Fernandez-Blanco, D., Bertotti, G., Schildgen, T.F., Garcin, Y., Strecker, M.R., Sudo, M., 2013. Plio-Quaternary Extensional Tectonics of the Central Anatolian Plateau: A case study from the Tuz Gölü Basin, Turkey, Turkish Journal of Earth Sciences, 22, 691-714.

Öztürk, Y.Y., Helvacı, C., Satır, M., 2012. Geochemical and Isotopic Constraints on Petrogenesis of the Beypazarı Granitoid, NW Ankara, Western Central Anatolia, Turkey, Turkish Journal of Earth Science, 21, 53-77.

Piper, J.D. a., Tatar, O., Gürsoy, H., 1997. Deformational behaviour of continental lithosphere deduced from block rotations across the North Anatolian fault zone in Turkey. Earth Planet. Sci. Lett. https://doi.org/10.1016/S0012-821X(97)00103-9

Piper, J.D.A., Gürsoy, H., Tatar, O., Beck, M.E., Rao, A., Koçbulut, F., Mesci, B.L., 2010. Distributed neotectonic deformation in the Anatolides of Turkey: A palaeomagnetic analysis. Tectonophysics 488, 31–50. https://doi.org/10.1016/j.tecto.2009.05.026

Piper, J.D.A., Moore, J.M., Tatar, O., Gürsoy, H., Park, R.G., 1996. Palaeomagnetic study of crustal deformation across an intracontinental transform: the North Anatolian Fault Zone in Northern Turkey, in: Morris, A., Tarling, D.H. (Eds.), Palaeomagnetism and Tectonics of the Mediterranean Region. Geological Society of London Special Publication, pp. 299–310.

Pourteau,A., M. Sudo, O. Candan, P. Lanari, O. Vidal, R. Oberhansli, 2013. Neotethys closure history of Anatolia: insights from 40 Ar–39 Ar geochronology and P–T estimation in high-pressure metasedimentary rocks, Journal of Metamorphic Geol., 31, 585–606.

Pourteau, A., 2011. Closure of the Neotethys Ocean in Anatolia: structural, petrologic and geochronologic insights from low-grade high-pressure metasediments, Afyon Zone, PhD Thesis. Potsdam University, 106 p.

Reches, Z., 1987. Determination Of The Tectonic Stress Tensor From Slip Along Faults That Obey The Coulomb Yield Condition. Tectonics 6, 849–861.

Reilinger, R., McClusky, S., Vernant, P., Lawrence, S., Ergintav, S., Cakmak, R., Nadariya, M., Hahubia, G., Mahmoud, S., Sakr, K., ArRajehi, A., Paradissis, D., Al-Aydrus, A., Prilepin, M., Guseva, T., Evren, E., Dmitritsa, A., Filikov, S. V, Gomes, F., Al-Ghazzi, R., Karam, G., 2006. GPS constraints on continental deformation in the Africa-Arabia-Eurasia continental collision zone and implications for the dynamics of plate interactions. J. Geophys. Res. 111, V05411, doi:10.1029/2005JB004051.

Rice, S.P., Robertson, A.H.F., Ustaömer, T., 2006. Late Cretaceous-Early Cenozoic tectonic evolution of the Eurasian active margin in the Central and Eastern Pontides, northern Turkey, Journal of the Geological Society of London Special Publications, 260, 413-445.

Rice, S.P., Roberson, A.H.F., Ustaömer, T., İnan, T., Taslı, K., 2009. Late Cretaceous-Early Eocene tectonic development of the Tethyan Suture Zone in the Erzincan area, eastern Pontides, Turkey. Geological Magazine, 146(4), 567-590.

Rigo de Righi, M., Cortesini, A., 1959. Regional studies in central Anatolian basin. Progress Report 1, Turkish Gulf Oil Co., Pet. İş. Gen. Md., Ankara.

Schildgen, T. F., D. Cosentinob., B. Bookhagen., S. Niedermann., C.Yıldırım., H. Echtlere., H. Wittmann., M.R. Strecker. 2012. Multi-phased uplift of the southern margin of the Central Anatolian plateau, Turkey: a record of tectonic and upper mantle processes. Earth Planet. Sci. Lett. 317–318, 85–95.

Schildgen, T. F., Yıldırım, C., Cosentino, D., Strecker, M. R., 2014. Linking slab break off, Hellenic trench retreat and uplift of the Central and Eastern Anatolian plateaus. Earth Sci. Rev. 128, 47–168.

Speciale, P.A., Catlos, E.J., Yıldız, G.O., Shina, T.A., Black, K.N., 2014. Zircon ages from the Beypazarı granitoid pluton (north central Turkey): tectonic implications, Geodinamica Acta, 25:3-4, 162-182.

Şengör, A.M.C., Görür, N., Şaroğlu, F., 1985. Strike-slip faulting and related basin formation in zones of tectonic escape: Turkey as a case study, in: Biddle, K.T., Christie-Blick, N. (Eds.), Basin Formation and Sedimentation. Society of Economic Paleontologists and Mineralogists Special Publications, pp. 227–264.

Tatar, O., Piper, J.D.A., Park, R.G., Gürsoy, H., 1995. Palaeomagnetic study of block rotations in the Niksar overlap region of the North Anatolian Fault Zone, central Turkey. Tectonophysics 244, 251–266.

Tüysüz, O., Dellaloğlu, A.A., Terzioğlu, N., 1995. A magmatic belt within the Neo-Tethyan suture zone and its role in the tectonic evolution of Northern Turkey, Tectonophysics, 243, 173-191.

Tüysüz, O., Tekin, U.K., 2007. Timing of imbrication of an active continental margin facing the northern branch of Neotethys, Kargı Massif, northern Turkey, Cretaceous Research, 28, 754-764.

van Hinsbergen, D.J.J., Kaymakcı, N., Spakman, W., Torsvik, T.H., 2010. Reconciling the geological history of western Turkey with plate circuits and mantle tomography. Earth Planet. Sci. Lett. 297, 674–68.

Wallace, R.E., 1951. Geometry of Shearing Stress and Relation to Faulting. The Journal of Geology, Vol. 59, No. 2 (Mar., 1951), pp. 118-130.

Whitney, D.L., Teyssier, C., Fayon, A.K., Hamilton, M.A., Heizler, M., 2003. Tectonic controls on metamorphism, partial melting and intrusion: timing and duration of regional metamorphism and magmatism in the Nigde Massif, Turkey, Tectonophysics, 376, 37-60.

Will, T.M., Powell, R., 1991. A robust approach to the calculation of paleostress fields from fault plane data. Journal of Structural Geology, 13, 813-821.

Yıldırım, C., Sarıkaya, M. A., Çiner, A., 2016. Late Pleistocene intraplate extension of the Central Anatolian Plateau, Turkey: inferences from cosmogenic exposure dating of alluvial fan, landslide and moraine surfaces along the Ecemiş Fault Zone. Tectonics 35, https://doi.org/10.1002/2015TC004038

Žalohar, J., Vrabec, M., 2007. Paleostress analysis of heterogeneous fault-slip data: the Gauss method. Journal of Structural Geology, 29, 1798–1810.

Appendix A. Field photos of fault plane measurement sites.

Ek A. Fay düzlemi ölçüm yerlerinden arazi fotoğrafları.

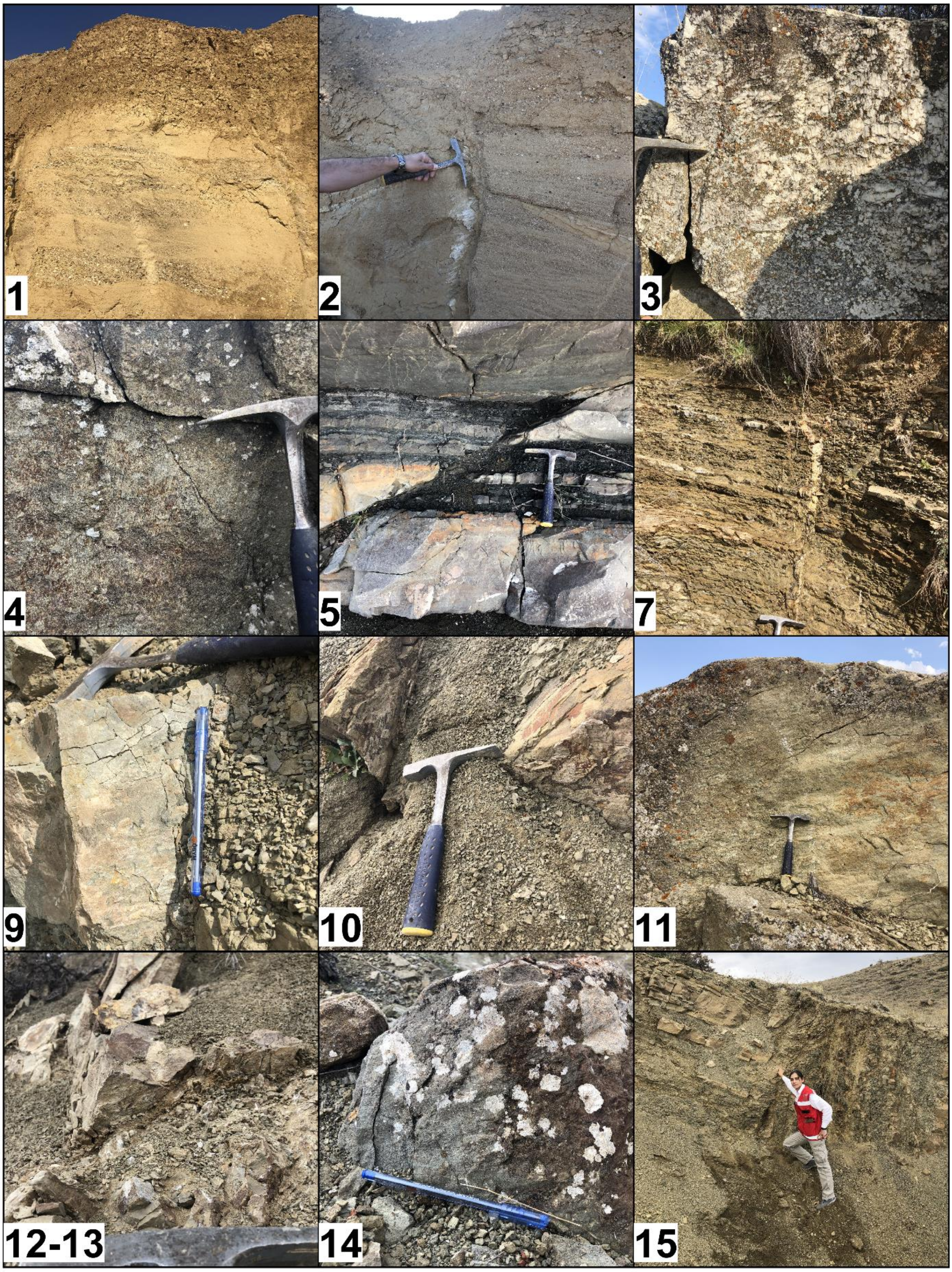

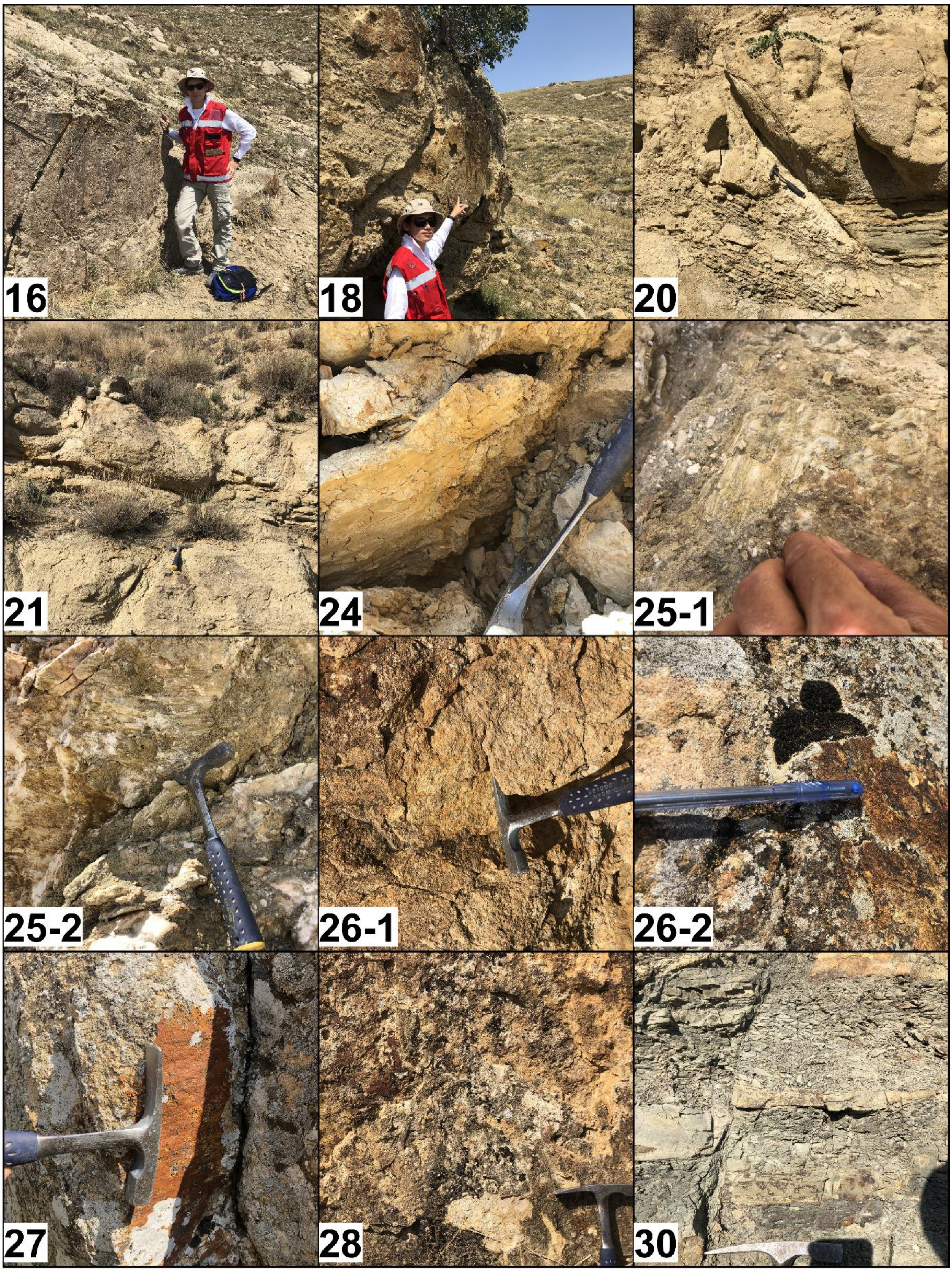
16
18
20
21
24
25-1
25-2
26-1
26-2
27
28
30

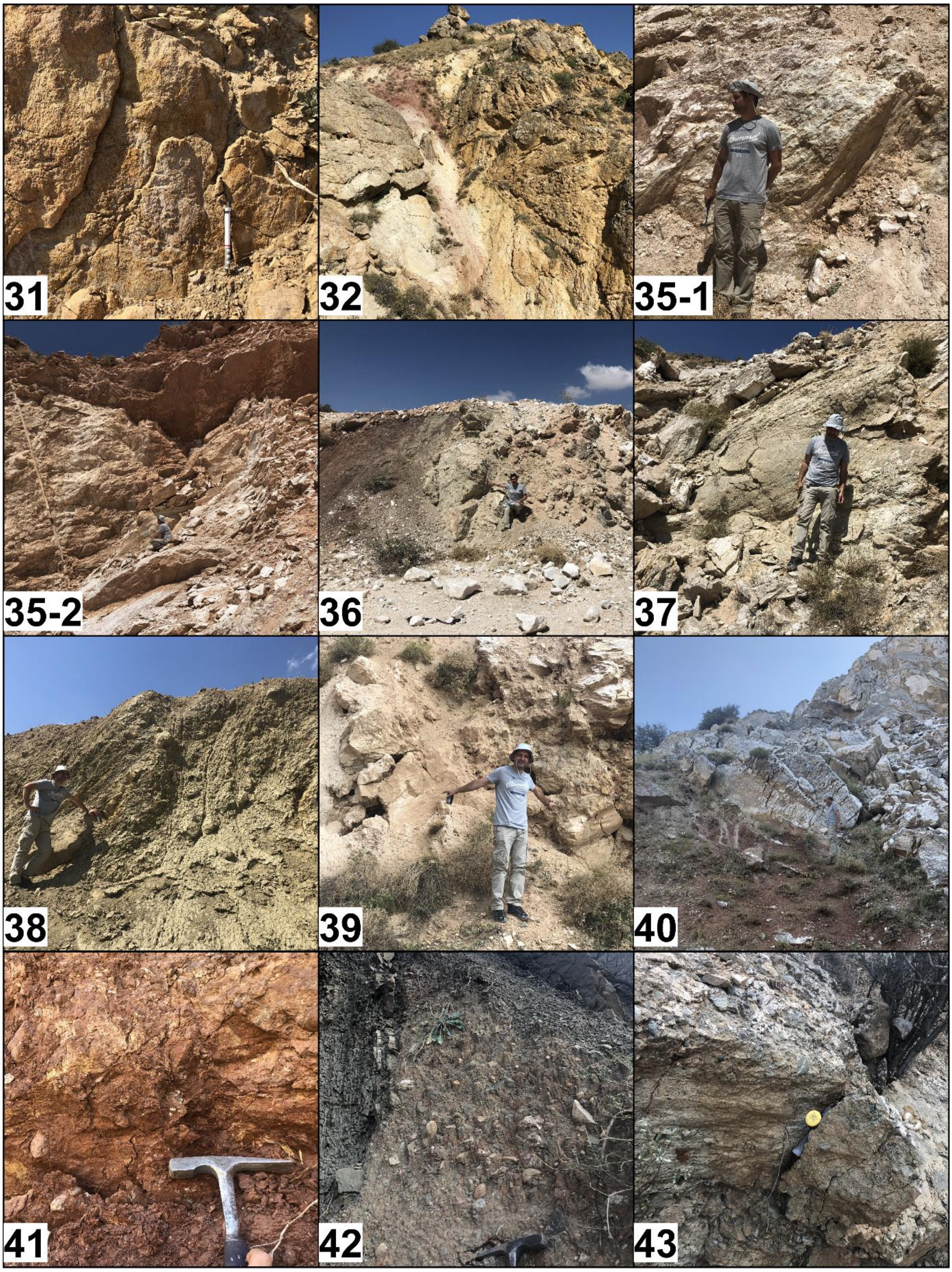
31
32
35-1
35-2
36
37
38
39
40
41
42
43

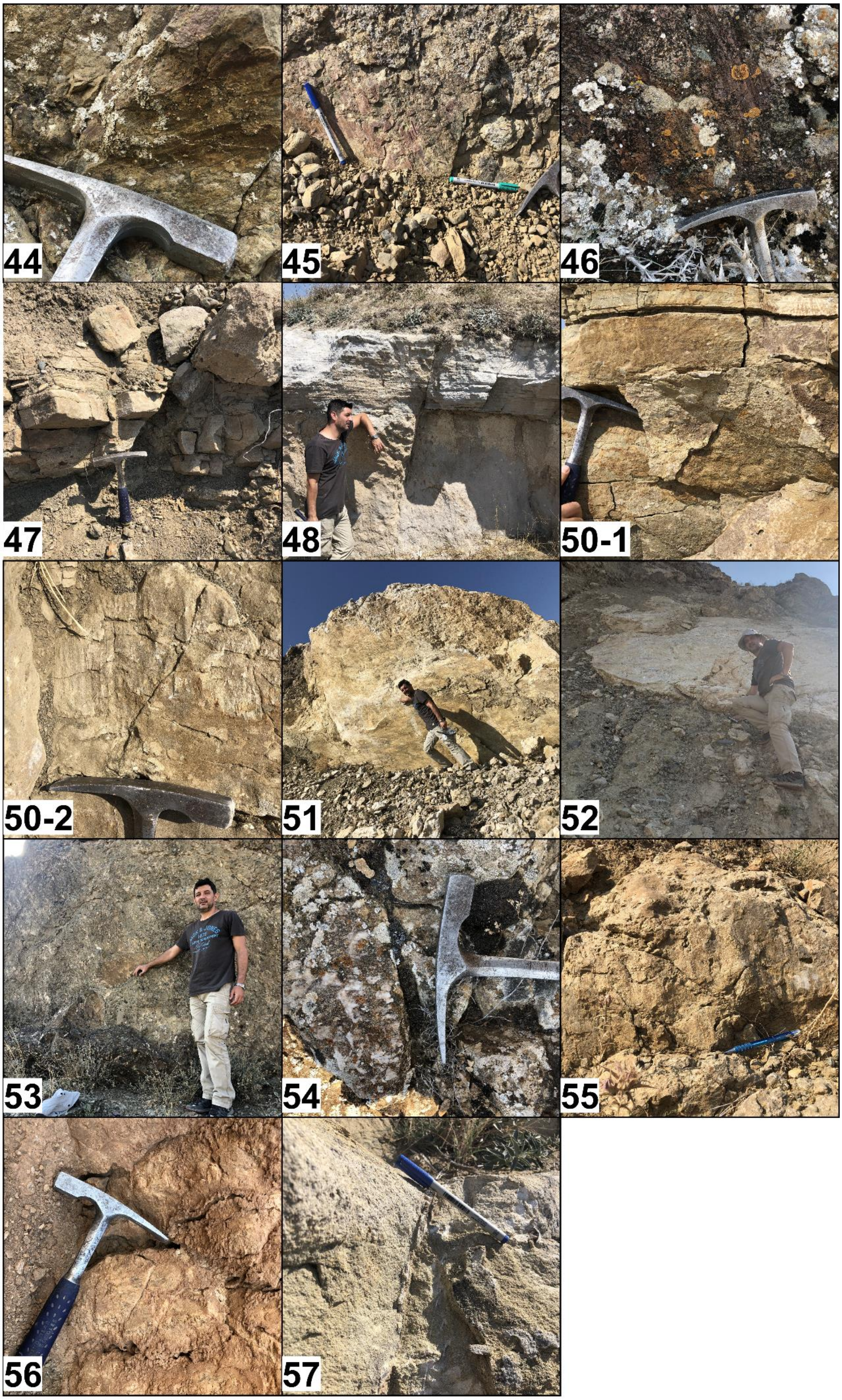
44
45
46
47
48
50-1
50-2
51
52
53
54
55
56
57

Appendix B. Locations and orientations of layers measured in the field.

Ek B. Arazide ölçülen tabaka konumları ve yerleri.

Latitude	Longitude	Dip	Dip azimuth
33.756	*38.661*	*45*	*245*
33.758	38.656	62	240
33.493	38.988	15	34
33.491	38.987	38	40
33.654	38.776	45	251
33.664	38.783	29	113
33.518	38.974	89	75
33.425	38.86	25	203
33.655	38.839	39	276
33.736	38.689	70	83
33.489	38.998	30	66
33.486	38.993	20	89
33.488	38.992	34	135
33.489	38.991	26	158
33.481	38.991	15	132
33.483	38.99	18	86
33.485	38.99	20	46
33.488	38.989	18	30
33.488	38.988	20	53
33.488	38.985	28	301
33.495	38.988	34	157
33.492	38.983	18	316
33.494	38.982	18	267
33.522	38.969	88	20
33.531	38.97	81	35
33.538	38.968	58	46
33.531	38.965	57	42
33.528	38.964	55	245
33.525	38.959	54	292
33.53	38.96	52	183
33.614	38.99	37	37
33.613	38.976	36	61
33.635	38.974	7	28
33.678	38.955	32	5
33.672	38.951	44	339
33.694	38.948	45	230
33.697	38.948	62	187
33.691	38.942	61	201
33.679	38.941	59	199
33.683	38.938	31	160
33.508	38.839	61	217
33.644	38.957	15	28
33.578	38.946	28	217
33.584	38.946	27	237
33.59	38.948	26	21
33.564	38.953	39	49
33.565	38.948	8	210
33.569	38.944	29	47
33.565	38.944	7	197
33.57	38.943	30	27
33.55	38.939	2	210
33.564	38.933	15	85
33.566	38.932	16	162
33.572	38.934	17	58
33.543	38.941	20	37
33.544	38.942	21	237
33.544	38.942	22	218
33.545	38.943	23	218
33.545	38.944	24	8
33.546	38.945	25	242
33.412	38.865	17	205
33.422	38.864	40	259
33.422	38.862	34	223
33.423	38.862	13	200
33.424	38.861	15	227
33.427	38.863	22	289
33.429	38.862	20	276
33.431	38.861	52	38
33.425	38.857	30	28
33.427	38.856	28	28
33.416	38.853	48	54
33.419	38.852	33	232
33.439	38.853	47	214
33.45	38.851	37	220
33.45	38.85	15	205
33.462	38.849	23	31
33.466	38.848	28	36
33.465	38.846	37	217
33.468	38.843	15	259
33.47	38.843	15	264
33.472	38.838	30	27
33.48	38.838	24	39
33.481	38.85	12	228
33.485	38.848	17	228
33.491	38.843	25	214
33.493	38.841	21	225
33.493	38.839	32	201
33.498	38.836	60	211
33.492	38.833	10	163
33.503	38.84	20	187
33.51	38.841	58	209
33.512	38.844	11	205
33.515	38.84	15	217
33.517	38.843	16	206
33.522	38.835	16	218
33.52	38.833	19	232
33.505	38.834	17	217
33.502	38.823	87	59
33.501	38.818	21	211

Latitude	Longitude	Dip	Dip azimuth
33.507	38.823	28	55
33.51	38.815	21	230
33.508	38.813	24	256
33.512	38.811	28	232
33.517	38.828	32	213
33.52	38.826	15	254
33.523	38.818	13	34
33.532	38.82	30	207
33.538	38.821	20	229
33.536	38.817	15	228
33.546	38.822	22	210
33.541	38.814	14	224
33.545	38.814	15	242
33.519	38.805	32	233
33.516	38.8	15	50
33.647	38.839	48	70
33.524	38.79	39	323
33.535	38.787	30	281
33.64	38.883	31	27
33.603	38.844	68	141
33.609	38.842	80	330
33.609	38.839	44	299
33.611	38.833	82	321
33.612	38.831	53	254
33.618	38.837	16	205
33.622	38.836	23	222
33.615	38.852	53	221
33.617	38.848	46	227
33.627	38.853	50	231
33.626	38.85	51	223
33.63	38.851	45	228
33.632	38.853	46	226
33.636	38.855	8	71
33.645	38.869	7	61
33.645	38.858	39	164
33.627	38.843	51	243
33.631	38.843	45	240
33.632	38.841	30	214
33.632	38.838	45	41
33.636	38.838	43	225
33.64	38.839	47	237
33.644	38.838	45	140
33.638	38.834	45	234
33.633	38.834	44l	291
33.635	38.829	55	250
33.637	38.83	40	252
33.638	38.829	60	163
33.642	38.834	68	156
33.641	38.832	31	112
33.64	38.829	72	139
33.628	38.826	50	270
33.632	38.822	33	305
33.629	38.821	30	260
33.628	38.818	40	326
33.633	38.819	55	318
33.631	38.815	44	140
33.63	38.812	45	276
33.633	38.813	20	125
33.629	38.809	24	134
33.632	38.806	23	132
33.637	38.804	43	70
33.64	38.809	47	125
33.639	38.822	42	96
33.639	38.816	62	133
33.639	38.8	35	300
33.639	38.793	42	296
33.641	38.796	57	290
33.644	38.798	39	337
33.758	38.658	36	258
33.667	38.82	20	217
33.645	38.801	29	335
33.645	38.803	30	286
33.648	38.801	49	330
33.652	38.804	28	262
33.652	38.796	24	305
33.646	38.793	45	308
33.651	38.789	40	309
33.651	38.791	30	313
33.656	38.809	24	247
33.659	38.806	53	286
33.667	38.808	64	322
33.668	38.804	63	291
33.656	38.848	40	131
33.651	38.839	34	65
33.65	38.835	68	53
33.658	38.838	60	200
33.655	38.834	27	196
33.666	38.833	40	56
33.662	38.826	43	229
33.658	38.832	47	224
33.684	38.793	6	49
33.657	38.793	85	153
33.658	38.791	35	247
33.658	38.79	35	47
33.662	38.79	38	147
33.663	38.787	34	74
33.662	38.785	35	153
33.666	38.786	10	96
33.664	38.768	25	185

Latitude	Longitude	Dip	Dip azimuth
33.666	38.765	66	11
33.665	38.761	30	50
33.67	38.762	35	258
33.671	38.762	30	238
33.672	38.761	44	261
33.671	38.759	41	252
33.672	38.756	35	239
33.673	38.758	45	246
33.678	38.76	83	0
33.739	38.689	50	81
33.677	38.759	32	28
33.678	38.769	50	243
33.675	38.768	11	306
33.681	38.772	18	270
33.682	38.771	23	259
33.681	38.765	60	49
33.674	38.755	30	284
33.673	38.751	50	238
33.689	38.747	43	224
33.693	38.747	47	203
33.687	38.744	45	221
33.694	38.744	46	218
33.691	38.741	14	266
33.694	38.738	10	196
33.697	38.74	65	262
33.696	38.728	24	50
33.703	38.729	51	223
33.706	38.731	40	218
33.707	38.726	43	236
33.715	38.731	38	106
33.719	38.73	45	38
33.735	38.687	32	43
33.721	38.727	3	233
33.692	38.703	50	200
33.694	38.7	51	218
33.72	38.706	28	283
33.728	38.709	43	273
33.729	38.711	71	306
33.729	38.708	54	264
33.726	38.707	30	266
33.723	38.705	31	225
33.727	38.703	52	318
33.731	38.704	60	79
33.731	38.699	60	96
33.731	38.697	54	53
33.733	38.697	30	56
33.731	38.696	60	64
33.731	38.694	27	62
33.733	38.693	32	73
33.736	38.693	18	308
33.743	38.696	25	233
33.738	38.693	27	239
33.742	38.694	32	259
33.742	38.692	30	287
33.739	38.685	38	114
33.744	38.684	27	310
33.74	38.684	30l	45
33.745	38.684	21	286
33.748	38.685	24	144
33.743	38.68	40	43
33.744	38.679	28	48
33.749	38.678	35	276
33.745	38.675	30	271
33.748	38.676	35	260
33.749	38.673	31	278
33.748	38.671	32	290
33.749	38.67	30	314
33.751	38.667	40	291
33.756	38.663	37	251
33.755	38.662	52	268
33.755	38.66	42	291
33.768	38.648	26	263
33.765	38.647	26	316
33.771	38.648	77	74
33.771	38.646	82	77
33.761	38.655	46	65
33.776	38.647	35	50
33.816	38.583	50	261
33.816	38.574	52	63
33.819	38.571	35	74
33.824	38.568	55	76
33.431	38.845	35	40
33.778	38.646	70	48
33.793	38.63	36	88
33.797	38.624	24	18
33.788	38.623	27	16
33.554	38.958	34	23
33.546	38.958	74	252
33.551	38.959	70	4
33.541	38.978	60	292
33.782	38.634	35	53
33.784	38.632	30	25
33.788	38.628	88	269
33.785	38.626	54	264
33.79	38.626	54	278
33.789	38.625	36	299
33.772	38.647	71	61